

5G CHALLENGES : WAVEFORM DESIGN AND D2D COMMUNICATION

A THESIS SUBMITTED TO
THE GRADUATE SCHOOL OF
ENGINEERING AND NATURAL SCIENCES
OF ISTANBUL MEDIPOL UNIVERSITY
IN PARTIAL FULFILLMENT OF THE REQUIREMENTS FOR
THE DEGREE OF
MASTER OF SCIENCE
IN
ELECTRICAL, ELECTRONICS ENGINEERING AND CYBER SYSTEMS

By
Hengameh Takshi
July, 2018

5G challenges : Waveform design and D2D communication

By Hengameh Takshi

July, 2018

We certify that we have read this thesis and that in our opinion it is fully adequate, in scope and in quality, as a thesis for the degree of Master of Science.



Prof. Dr. Hüseyin Arslan(Advisor)

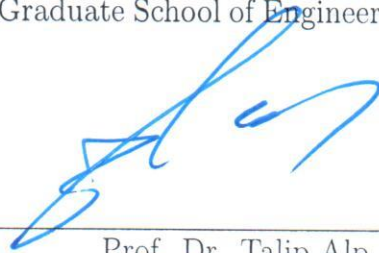


Assoc. Prof. Dr. Hasari Çelebi



Assist. Prof. Dr. Tuncer Baykaş

Approved by the Graduate School of Engineering and Natural Sciences:



Prof. Dr. Talip Alp

Director of the Graduate School of Engineering and Natural Sciences

I hereby declare that all information in this document has been obtained and presented in accordance with academic rules and ethical conduct. I also declare that, as required by these rules and conduct, I have fully cited and referenced all material and results that are not original to this work.

Name, Last Name: HENGAMEH TAKSHI

Signature

: 

ABSTRACT

5G CHALLENGES : WAVEFORM DESIGN AND D2D COMMUNICATION

Hengameh Takshi

M.S. in Electrical, Electronics Engineering and Cyber Systems

Advisor: Prof. Dr. Hüseyin Arslan

Co-Advisor: Assoc. Prof. Dr. Gülüstan Doğan

July, 2018

Fifth generation (5G) of communication systems is expected to satisfy a wide variety of requirements with regards to different applications. Flexibility, low latency, low power consumption are the most important ones. Using another waveform other than orthogonal frequency division multiplexing (OFDM) waveform which avoids the disadvantages of OFDM can help to satisfy the requirements. In the literature, there are multiple research works about proposing new waveform. One of the most important thing which needs to be satisfied by the 5G waveform is the flexibility. The first part of the thesis is focused on the proposing two flexible waveform. The first proposed waveform is DFT-s- ZW OFDM which has similar transceiver to ZT DFT-s-OFDM. In DFT-s-ZW OFDM instead on zeros in ZT DFT-s-OFDM in time domain we create those zeros at the tail of output of IFFT. With this approach the flexibility of ZT DFT-s-ODM in terms of guard interval length is kept but the problem of ISI is solved.

Device-to-Device (D2D) communication plays an important role in the next generation of communication systems. Enabling D2D communication decreases latency and expands the coverage of a cell in cellular networks. Additionally, D2D underlying cellular users benefits from high spectral efficiency. However, it creates interference to cellular communications. In the second part of this thesis, we propose a genetic algorithm-based method to minimize the interference and maximize the spectral efficiency. One of the advantages of genetic algorithm is that it escapes from local maximums and evolves toward global maximum by searching different parts of search space simultaneously. Since D2D underlay cellular network degrades the signal to interference plus noise ratio (SINR), a

minimum SINR is considered for cellular users. Numerical evaluations demonstrate the superior performance of the proposed technique in terms of spectral efficiency and interference mitigation.

In wireless networks, the need for accurate and low complexity localization methods are growing. Although many positioning methods based on signals' time difference of arrival (TDOA) and angle of arrival (AOA) have been proposed, these methods require multiple base stations (BS) and calculations with high complexity. Furthermore, the distance between a target and the BSs are usually larger than the distance between different BSs, which causes geometric dilution of precision (GDP) problem. In third part of this thesis, to circumvent these issues, we propose a novel and linear method for positioning by only one BS. Our method uses both AOA and TDOA of incoming signals and called "positioning using one BS (PuOB)". In this method, we take measurements from one BS at different time instances instead of taking measurements from multiple BSs simultaneously. The ability to estimate the mobile transmitter position accurately by using one BS is the highlighted advantage of the PuOB over the conventional methods. The positioning accuracy of PuOB for different BS numbers are presented. According to simulation results, PuOB outperforms TDOA and AOA methods using three and two BSs, respectively.

Keywords: Device to device communication, out of band emission, resource allocation, Spectral efficiency, Waveform.

ÖZET

5G ZORLUKLAR: DALGA BİÇİMİ TASARIMI VE D2D İLETİŞİMİ

Hengameh Takshi

Elektrik-Elektronik Mühendisliği ve Siber Sistemler, Yüksek Lisans

Tez Danışmanı: Prof. Dr. Hüseyin Arslan

Tez Eş Danışmanı: Doç. Dr. Gülüstan Doğan

Temmuz, 2018

Beşinci nesil (5G) iletişim sistemlerinin, farklı uygulamalarla ilgili çok çeşitli gereksinimleri karşılaması beklenmektedir. Esneklik, düşük gecikme, düşük güç tüketimi en önemli olanlardır. OFDM'nin dezavantajlarını ortadan kaldıran ortogonal frekans bölme (OFDM) dalga formundan başka bir dalga formu kullanmak, gereksinimlerin karşılanmasına yardımcı olabilir.

Cihazdan Ağıta (D2D) iletişim, gelecek nesil iletişim sistemlerinde önemli bir rol oynar. D2D iletişimini etkinleştirmek, gecikmeyi azaltır ve hücresele ağlarda bir hücrenin kapsamını genişletir. Ek olarak, D2D'nin hücresele kullanıcıları desteklemesi, yüksek spektral verimden faydalanır. Ancak, hücresele haberleşmelere müdahale oluşturur.

Kablosuz ağlarda, doğru ve düşük karmaşıklık yerleştirme yöntemlerine olan ihtiyaç artmaktadır. Her ne kadar sinyallerin 'varış zamanı (TDOA) ve varış açısı (AOA)' na dayanan birçok konumlandırma yöntemi önerilmişse de, bu yöntemler çoklu baz istasyonları (BS) ve yüksek karmaşıklık gerektiren hesaplamalar gerektirir.

Anahtar sözcükler: Cihazdan cihaza haberleşme, bant dışı çıkış, kaynak tahsisi, spektral verim, dalga biçimi.

Acknowledgement

I would first like to thank my thesis advisor Prof. Hüseyin Arslan of the Istanbul Medipol University. The door to Prof. Arslan office was always open whenever I ran into a trouble spot or had a question about my research or writing. He consistently allowed this paper to be my own work, but steered me in the right the direction whenever he thought I needed it. I would also like to thank my co-advisor Dr. Gülüstan Doğan for her excellent advice and support. Her efforts in providng me with constant feedback are greatly appreciated.

In addition, I want to express my heartfelt appreciation to my family and friends for their continuous encouragement and their moral support.

Contents

1	Introduction	1
1.1	5G waveform	1
1.2	Joint Optimization of Device to Device Resource and Power Allocation based on Genetic Algorithm	2
1.3	A Novel One-Base Station Hybrid Positioning Method	7
2	5G Waveforms	10
2.1	DFT-s-ZW-OFDM	10
2.2	A Flexible Hybrid Waveform	16
3	Joint Optimization of Device to Device Resource and Power Allocation based on Genetic Algorithm	22
3.1	System Model and Problem Formulation	22
3.2	Algorithm Description	26
3.2.1	Determining fitness function and power assignment	27
3.2.2	Proportional selection	28

3.2.3	Crossover operation	28
3.2.4	Mutation	29
3.2.5	Optimization using genetic algorithm operators	30
3.3	Channel prediction	30
3.4	Simulation Results	32
3.4.1	Network Spectral Efficiency Evaluation	33
3.4.2	CDF Evaluation	34
3.4.3	Interference Evaluation	35
4	A Novel One-Base Station Hybrid Positioning Method	45
4.1	System Description	45
4.1.1	Time Difference of Arrival (TDOA) Method	46
4.1.2	Angle of Arrival (AOA) Method	46
4.1.3	Positioning using One Base Station (PuOB) Method	47
4.2	Performance Evaluation	52
5	Concluding Remarks	56
5.1	Summary	56

List of Figures

1.1	Classification of D2D communication based on the spectrum sharing.	3
2.1	DFT Spread Zero Word OFDM	11
2.2	Transmitted signals in the time domain.	13
2.3	PAPR comparison without considering tails.	14
2.4	Power spectral density comparison.	15
2.5	Proposed hybrid waveform.	17
2.6	Co-locating ZW and ZT subcarriers without a guard between them.	18
2.7	Power evaluation. Trade-off between symbol power and tail power.	19
2.8	BER performance of the hybrid waveform in Rayleigh fading channel with uniform PDP distribution, $\tau = 21$	20
2.9	Power spectral density comparison.	21
3.1	A sample chromosome representation: RB_1 is shared by U_2, U_3 and U_4 with power of p_2, p_3 and p_4 , respectively. Also RB_2 is shared by U_1 and U_5 with power of p_1 and p_5 , respectively. $\mathbf{M} = \{U_1, U_2\}$ and $\mathbf{D} = \{U_3, U_4, U_5\}$ are cellular users and D2D pairs, respectively.	26

3.2	Crossover operation. Parent 1 and Parent 2 produce offspring. crossover point randomly is selected and equals to 2. Moreover, length of two resource blocks, which are randomly selected, equal to 4 and 1, respectively.	36
3.3	Spectral efficiency for different number of resource blocks.	40
3.4	Spectral efficiency with respect to the number of available resource blocks.	41
3.5	Spectral efficiency for different number of repetitions.	42
3.6	Cumulative distribution function of spectral efficiency.	43
3.7	Network interference for different number of repetitions.	44
4.1	Hyperbola made by TDOA measurements in two BSs located at \mathbf{S}_m and \mathbf{S}_{m-1} as foci and the target located at \mathbf{P}_n	48
4.2	The x-D antenna array of the m^{th} BS for measuring angle of arrival $\alpha_{m,n}$	48
4.3	The PuOB positioning of a target located at \mathbf{P}_n with one BS located at \mathbf{S}_m	50
4.4	Average localization error of PuOB, AOA and TAP methods, for different x,y locations of a target. (The height of the target, σ_{TDOA} and $[\sigma_\phi \ \sigma_\theta]^T$ are set to 1000 m, 30 ns and $[0.5 \ 0.5]^T$ degrees, respectively.)	51
4.5	Performance comparison of PuOB with different initializations, AOA and TAP localizations of a target located in y-axis while BSs are located in x-axis.	53

4.6 The effect of σ_{TDOA} variation on the performance of PuOB, AOA and TAP methods. 53

4.7 The effect of $[\sigma_\phi \ \sigma_\theta]^T$ variations on the performance of PuOB, AOA and TAP methods ($\sigma_\phi = \sigma_\theta$). 55

List of Tables

3.1 System Numerical Parameters	32
---	----

Chapter 1

Introduction

1.1 5G waveform

Fifth generation (5G) of mobile communication demands for a faster (low latency) and more flexible with a higher capacity mobile communication. In order to achieve this, waveform design can help a lot. Orthogonal frequency division multiplexing (OFDM), as fourth generation waveform has lots of advantages but suffers from a number of disadvantages such as large out of band (OOB) emission and peak to average power ratio (PAPR). Also, requiring a fixed cyclic prefix (CP) in a system makes OFDM not flexible for most of 5G scenarios. These disadvantages motivate researchers to propose a new waveform which satisfies the requirements.

Some OFDM-based waveforms have been proposed for 5G in order to overcome these drawbacks; however, they have their own disadvantages. A waveform like filter-bank-multi-carrier (FBMC) [19], although has a high spectral efficiency, it has long length filtering which increases latency for short data bursts. Also the use of OQAM modulation makes it inappropriate to adapt with different schemes in 5G. Universal filtered multi-carrier (UFMC) can be considered as a generalized form of filtered-OFDM (f-OFDM) [34],[41]. It has good OOB emission, but requiring zero guard (ZG) between symbols in time domain and having intercarrier

interference (ICI) in small groups of subcarriers are its disadvantages. DFT-s-OFDM is currently used in LTE-uplink [6] has good PAPR but still needs CP and has large OOB emission.

For a system with time varying channel, a fixed length CP does not work. However, having different CP lengths in one system destroys orthogonality between OFDM symbols. Therefore, a flexible CP is heavily required.

1.2 Joint Optimization of Device to Device Resource and Power Allocation based on Genetic Algorithm

Next generation of mobile communication systems comprises of wide variety of applications. Internet of things (IoT) is one of these applications that connects a tremendous number of devices and users to each other [53]. By increasing the number of IoT-based applications, communicating through a base station (in cellular network) imposes a huge load on the network. It also increases the latency of the communication and decreases the quality of service. Device to device (D2D) communication is proposed to overcome these problems. This type of communication allows the nearby devices to communicate directly, independent of base station, to each other [5, 9, 29]. Therefore, D2D communication decreases the load of the network and expands the coverage of the base station by enabling multi-hop transmission.

D2D communication in spite of simplicity has some challenges. Choosing the spectrum for D2D communications is one of the challenges[37, 33]. Based on the used spectrum by D2D users and their impact on the cellular users, D2D communication can be classified as shown in Figure 1.1 [4]. One approach is that D2D users use unlicensed spectrum such as TV white space[26, 50]. In this case, there is no interference from D2D users to cellular users using licensed spectrum and

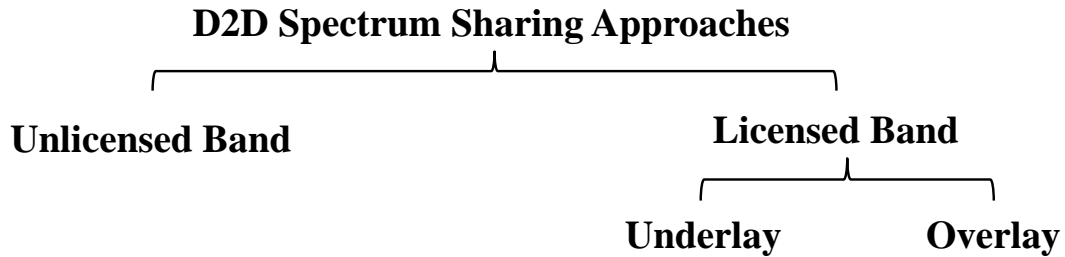


Fig. 1.1: Classification of D2D communication based on the spectrum sharing.

vice versa. However, due to the limited rules over the unlicensed spectrum, it is difficult to control it and usually not preferable. The other approach is that D2D users along with cellular users utilize the licensed spectrum [25]. This category is also classified into two subgroups of overlay and underlay. In overlay, the D2D users and cellular users utilize orthogonal time/frequency resource blocks (i.e. the smallest unit of resources that can be allocated to a user) [51, 8]. In other words, the resources are divided into two groups, one for cellular users and the other one for D2D users. Due to the orthogonality of the resources, there is no interference from one user to other users. However, in the overlay, the spectrum is not utilized efficiently, because there might be some unused resources in one group while there are not enough resources in the other group. Despite the overlay, in underlay, D2D users utilize the same spectrum as the cellular users [13, 48, 49, 54, 47]. Therefore, more users can be served within a fixed spectrum compared to the overlay. Note that although the spectrum is used more efficiently in underlay, there is interference between the communications who share the same resource blocks. Thus, the importance of an interference management and intelligent resource allocation method is increased. Interference mitigation results in efficient spectrum utilization.

In the literature, a significant effort has been done related to the resource allocation and interference mitigation in underlay D2D communication [49, 54, 47, 40, 39, 52, 1, 21, 2, 22, 36, 38, 44, 45]. In [49], the authors presented a joint mode selection, channel assignment and power control to maximize the spectral efficiency. They proposed three different modes under which a D2D pair can either reuse a resource of a cellular user or use a dedicated resource. In the case

of reusing, only one D2D pair shares a resource block with a cellular user which restrict the number of served userd. In the other hand, the maximization is done in two steps: 1) power control 2) channel assignment. These two steps are done independently which results in not a very optimized solution.

In [54], a greedy algorithm is proposed for resource allocation for D2D underlaying cellular networks. The authors assumed that the number of cellular users is larger than the D2D pairs which is not a realistic assumption for the new generation of communications. In [47], another greedy algorithm is presented which is used only for resource allocation. However, the users either transmit with the maximum power or they do not have a transmission. In other words, the effect of transmission power on the interference is not considered. Also, the authors assumed that a single pair of D2D users can only share the resource block with a cellular user. Thus, the number of served users is also limited. Furthermore, the greedy algorithms often stuck in local optimum solutions and do not evolve toward the global optimum solutions.

The purpose of the resource allocation in [40] is to have longer battery life at each device. Resource allocation is done to enable the users to transmit with a minimum power. However, efficient spectrum usage is not considered. In [39], another resource allocation method for increasing the energy efficiency and battery life of user equipment is suggested. For this purpose, an iterative combinatorial auction algorithm is used where D2D pairs and cellular users are as bidders and auctioneer, respectively.

Authors in [52] suggested to use different algorithms for resource allocation in multiple input multiple output (MIMO) systems under different conditions. First, they proposed an algorithm based on random search that search a huge search space randomly for finding a sub-optimal solution. Then, the use of game theory is suggested for the cases that users has incomplete information. Moreover, an iterative algorithm based on best response dynamic structure and an algorithm using sum-rate reinforcement mechanism is proposed as alternatives for solving

the game theoretic problem.

In [1], authors minimized the interference while maximizing the spectral efficiency using only resource allocation and does not consider transmission power. Moreover, only one D2D pair is allowed to share a resource block with a cellular users.

Authors in [21], used resource allocation done by a proposed two-phased algorithm, to minimize the interference for a given spectral efficiency. Thus, the result is not the optimum solution in terms of spectral efficiency.

Authors in [2] aimed to maximize spectral efficiency per unit network power consumption. Authors formulated the optimization problem as a non-linear fractional programming problem. Then, They converted it to the concave optimization problem using Charnes-Cooper transformation. In order to solve the concave optimization problem outer approximation algorithm is proposed. Therefore, in [2] maximizing the over all spectral efficiency is not considered.

In [22], the authors suggest minimizing the interference from D2D users to the cellular by decreasing the power of D2D users, and the interference from the cellular users to D2D users by choosing the best resource. In their research one resource block can be shared with one cellular user and one device to device user at most, which can prevent using the resources efficiently.

In [36], multiple different game algorithms for resource allocation are presented. The non-cooperative and cooperative behaviors of mobile users are analyzed to control the transmission power for underlay D2D communication. Then, the power control is done by a non-cooperative static game profiting from Game theory. Additionally, Stackelberg game is used for resource allocation while the

resources for cellular users are assumed to be known. Authors also proposed combinatorial auction for resource allocation of both cellular users and D2D users. However, a suitable resource allocation highly depends on the transmission power of the user. Therefore, since the resource allocation is done independent of the power control, the result is not well-optimized.

Stackelberg game is also suggested in [38] to coordinate the resource allocation and power assignment. The authors used the downlink resources. However, due to the heavy load of download links and high power of base station, sharing downlink resources is not preferable. Also sharing a cellular user resource block with only one D2D pair is considered which restricts the number of served users.

In [44], authors suggested to use sequential second price auction as a method for resource allocation. However, the result is not an optimal solution because in the resource allocation, the effect of assigning different resources to cellular users is not considered. In other words, the resource allocation for cellular users is done before the optimization.

In [45], a genetic algorithm-based joint resource allocation and user matching scheme (GAAM), is proposed. Genetic algorithm, unlike the greedy algorithms, escapes from the local maximums by adding some randomness to the search space. The probability of the added randomness should be small. Otherwise, the search gets similar to a random search. However, huge mandatory randomness is added in the algorithm in [45] which degrades the performance of the algorithm. Also, GAAM shares a resource block of a cellular user with only one D2D pair without power control.

All of the mentioned algorithms are in the category of the interference aware algorithms. They require knowledge of global channel state information (CSI) between different pairs at all the transmission time intervals (it is usually obtained

by feedback from users to base station). Achieving this information causes a huge load on the network. Although authors in [54, 47, 40, 39, 52, 1, 21, 2, 38, 44, 45] did not highlight this problem, a periodically update method for CSI is suggested in [22]. However, it makes the information not useful due to delay caused by feedback or collecting the information periodically which affects the performance of the algorithms. Also in [36], a method based on local CSI is proposed, but in the next generation of communications, there is a huge number of users and devices even in local areas. Therefore, the number of channels required to be known and imposed load due to it are still huge.

In this chapter, we propose a joint optimization for resource allocation and power assignment based on the genetic algorithm to maximize the spectral efficiency of the network. Moreover, a minimum SINR for the cellular users is guaranteed. Also, there is no restriction on the number of D2D users that can share a resource block with a cellular user. Furthermore, in order to reduce the overhead of CSI knowledge, we suggest to use a channel prediction method to reduce the overhead significantly while the performance is preserved.

1.3 A Novel One-Base Station Hybrid Positioning Method

Positioning and tracking of mobile transmitters are important parts of new wireless navigation systems and cellular radio networks. A positioning method requires to satisfy the imposed requirements, such as high reliability and accuracy along with keeping the costs and complexity low. Methods based on time of arrival (TOA), time difference of arrival (TDOA), angle of arrival (AOA) and received signal strength (RSS) of the signals [20, 32, 30] are the most significant and well-known approaches.

The TOA method requires knowledge of the time instances that a signal is transmitted and received; on the other hand, TDOA requires only the time difference of arrivals at different receivers. In this study, we mainly focus on cellular networks thus Base Stations (BS) are considered as receivers. It is worth mentioning that both TOA and TDOA methods need an accurate synchronization between different BSs which increases complexity of the methods. In [23] and [43], authors removed the need of synchronization between BSs by considering the location of mobile transmitter in two different time instances, while requiring the utilization of multiple BSs for the estimation of the location of the transmitter. The AOA method unlike the TOA and TDOA methods uses angles of received signal in different BSs. For AOA measurements, either directional antennas or antenna arrays at each BS are required [35]. Although AOA have some advantages over TDOA, it is not precise in non-line of sight (NLOS) scenarios thus TDOA is preferred more by systems designers [35]. RSS method is another method utilizing the known power of transmitted signal for positioning; however, its precision is less than the previous methods due to multipath fading [7].

For the mentioned methods number of BSs and cost are significant issues. The minimum number of required BSs that AOA and TDOA methods require for 3-dimensional (3-D) positioning are two and four BSs, respectively.

Recently, in [28, 46, 31] new methods are introduced, requiring at least two BSs to have an accurate estimation. The methods are inspired from previous positioning methods like AOA and TDOA. In [28], the authors proposed a method in which direction of the transmitter is estimated using TDOA while AOA method is used to have the initial range. Although the method given in [28] proposes a linear hybrid method and solves the non-convergence problem of TDOA utilizing AOA method, it does not consider number of BSs and cost. In [46], authors proposed a combined TDOA-AOA positioning (TAP) method. Measurements from AOA and TDOA and the unknown position of the transmitter are used to construct mathematical relations in order to find the unknown position. The performance of this method highly depends on AOA measurements. In [31], an approach based on AOA is proposed considering Doppler shift for positioning of a mobile source. Instead of estimating at the BSs, the unknown position is

estimated at the mobile target in [31]. The method requires LOS transmission like AOA method with using two BSs in 2-D coordinates. Consequently, it is necessary to have more BSs for 3D-positioning estimations.

In addition, most of the mentioned methods suffer from a problem called geometric dilution precision (GDP) happens when the distance of transmitter from BSs is more than distances between BSs. It causes to lose the precision in estimations or even make the position finding equations non-solvable [28]. Although some of the methods like the method in [28] try to decrease GDP problem, it increases the complexity and cost.

In this study, a novel positioning method is proposed to solve the mentioned restrictions in order to estimate the location of a distant mobile transmitter based on unknown received signal power at only one BS. Thus, there is no necessity of synchronization between different BSs. In addition, we propose a highly reliable positioning method called **positioning using one BS (PuOB)**. The new method is based on AOA and TDOA measurements which are taken at one BS in different time instances.

Chapter 2

5G Waveforms

2.1 DFT-s-ZW-OFDM

The transceiver of the proposed waveform is shown in Fig. 2.1. The transmitter is similar to the transmitter of DFT-s-OFDM. There is a difference between DFT and IFFT. In the proposed waveform, DFT-s-ZW-OFDM, some redundant subcarriers are added. The data on these subcarriers is calculated in a way that at the output of IFFT there is a zero word. The length of zero word is equal to number of redundant subcarriers. Because The size of the IFFT is fixed, the orthogonality is saved even with different size of zero word.

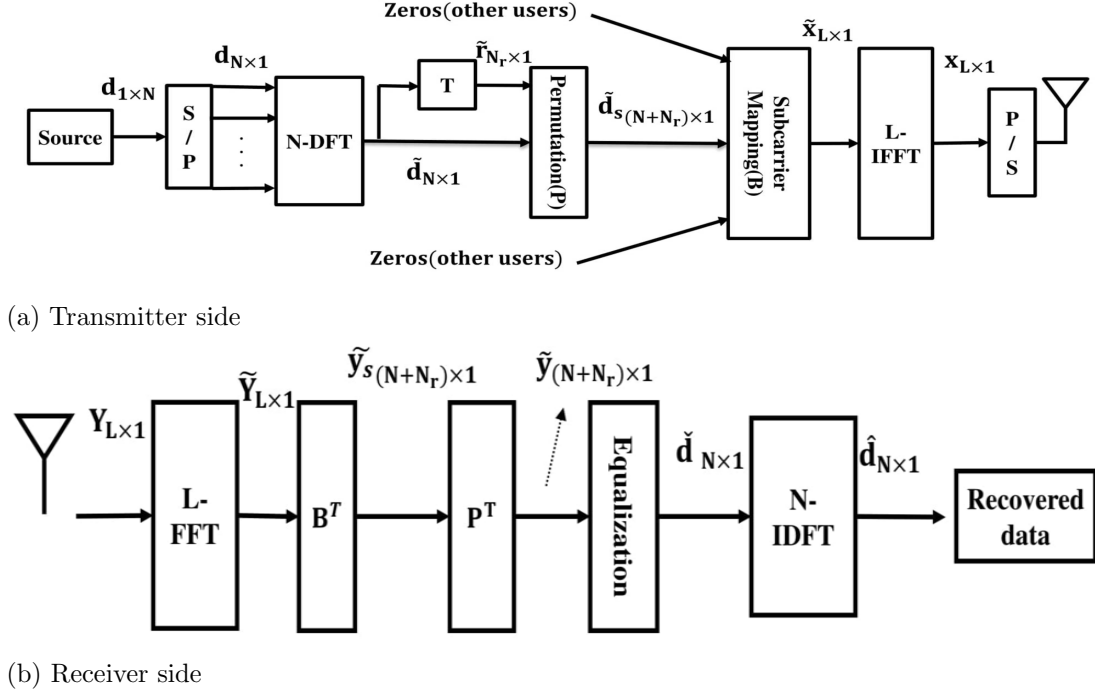


Fig. 2.1: DFT Spread Zero Word OFDM

The mathematical operations in DFT-s-ZW-OFDM can be summarized as

$$\tilde{\mathbf{d}}_{(N \times 1)} = \mathbf{D}_{(N \times N)} \times \mathbf{d}_{(N \times 1)}, \quad (2.1)$$

where $\mathbf{d}_{(N \times 1)}$, $\mathbf{D}_{(N \times N)}$ and $\tilde{\mathbf{d}}_{(N \times 1)}$ are data in time domain, DFT matrix and corresponding data in frequency domain, respectively.

$$\begin{aligned} \tilde{\mathbf{r}}_{(N_r \times 1)} &= \mathbf{T}_{(N_r \times N)} \times \tilde{\mathbf{d}}_{(N \times 1)} \\ &= \mathbf{T}_{(N_r \times N)} \times \mathbf{D}_{(N \times N)} \times \mathbf{d}_{(N \times 1)}. \end{aligned} \quad (2.2)$$

where $\tilde{\mathbf{r}}_{(N_r \times 1)}$ and $\mathbf{T}_{(N_r \times N)}$ are the redundant subcarriers and transformation matrix. Transformation matrix calculates the value on the redundant subcarriers based on the data. Then, redundant subcarriers are permuted between the data subcarriers using $\mathbf{P}_{(N+N_r) \times (N+N_r)}$ all the subcarriers (redundant and data subcarriers) are mapped to the IFFT using a mapping matrix called $\mathbf{B}_{L \times (N+N_r)}$.

the output signal of the transmitter is named as \mathbf{x} and is calculated as:

$$\mathbf{x} = \mathbf{F}_L^{-1} \tilde{\mathbf{x}}_{L \times 1} = \overbrace{\mathbf{F}_L^{-1} \mathbf{B} \mathbf{P}}^{\mathbf{M}} \begin{bmatrix} \mathbf{I} \\ \mathbf{T} \end{bmatrix} \mathbf{D}_N \mathbf{d} \quad (2.3)$$

\mathbf{M} can be divided into four submatrices and can be written as $\mathbf{M} = \begin{bmatrix} \mathbf{M}_{11} & \mathbf{M}_{12} \\ \mathbf{M}_{21} & \mathbf{M}_{22} \end{bmatrix}$. As mentioned earlier the tail of output of the IFFT contains

zero there fore we can rewrite \mathbf{x} as $\begin{bmatrix} \mathbf{x}_{\text{non.tail}} \\ \mathbf{x}_{\text{tail}} \end{bmatrix} = \begin{bmatrix} \mathbf{x}_{\text{non.tail}} \\ 0 \end{bmatrix}$. We can have

$$\begin{bmatrix} \mathbf{x}_{\text{non.tail}} \\ 0 \end{bmatrix} = \begin{bmatrix} \mathbf{M}_{11(N \times N)} & \mathbf{M}_{12(N \times N_r)} \\ \mathbf{M}_{21(N_r \times N)} & \mathbf{M}_{22(N_r \times N_r)} \end{bmatrix} \begin{bmatrix} \mathbf{D}_N \mathbf{d} \\ \tilde{\mathbf{r}} \end{bmatrix}, \quad (2.4)$$

and $\tilde{\mathbf{r}}$ can be rewrite as

$$\tilde{\mathbf{r}} = -\mathbf{M}_{22}^{-1} \mathbf{M}_{21} \overbrace{\mathbf{D}_N \mathbf{d}}^{\tilde{\mathbf{d}}}. \quad (2.5)$$

Thus transformation matrix is

$$\mathbf{T} = -\mathbf{M}_{22}^{-1} \mathbf{M}_{21}. \quad (2.6)$$

Fig. 2.2 shows the transmitted signals in time domain for DFT-s-OFDM, ZT DFT-s-OFDM and DFT-s-ZW OFDM.

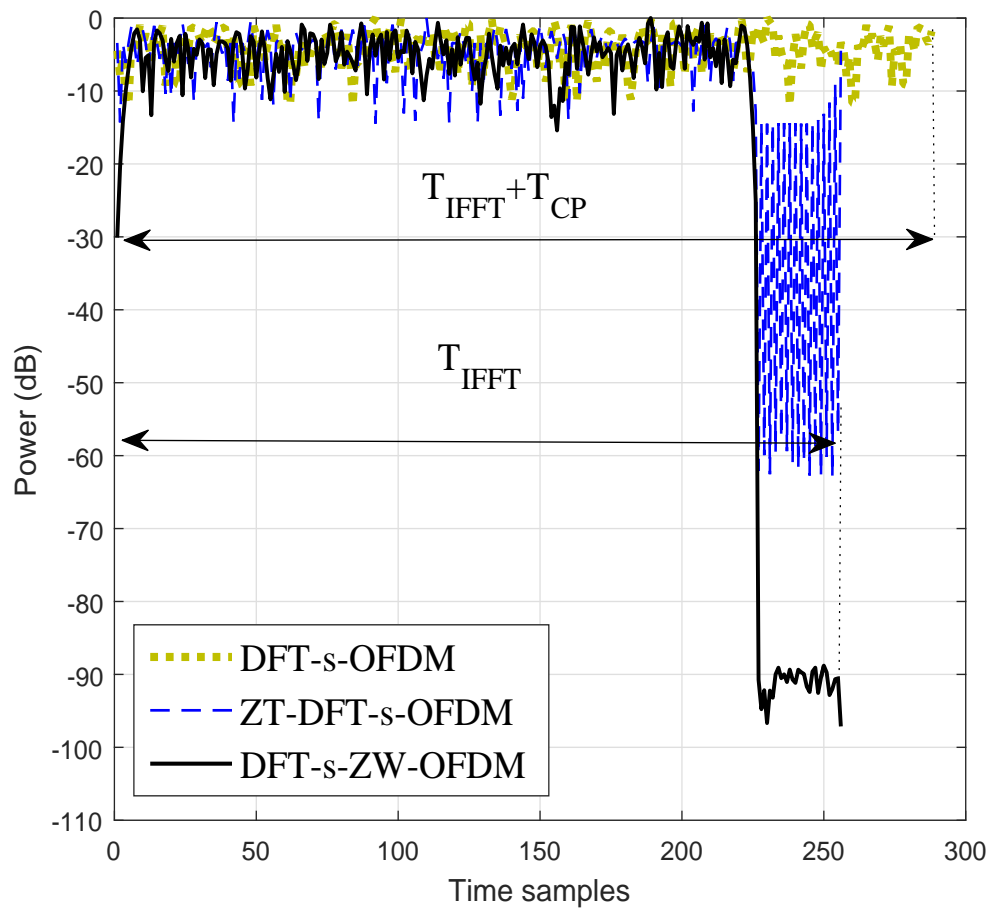


Fig. 2.2: Transmitted signals in the time domain.

The PAPR comparison between CP-OFDM, UW-OFDM, DFT-s-ZW-OFDM,

ZT-DFT-s-OFDM and DFT-s-OFDM is shown in Fig. 2.3. The redundant sub-carriers is the reason for the increase in PAPR.

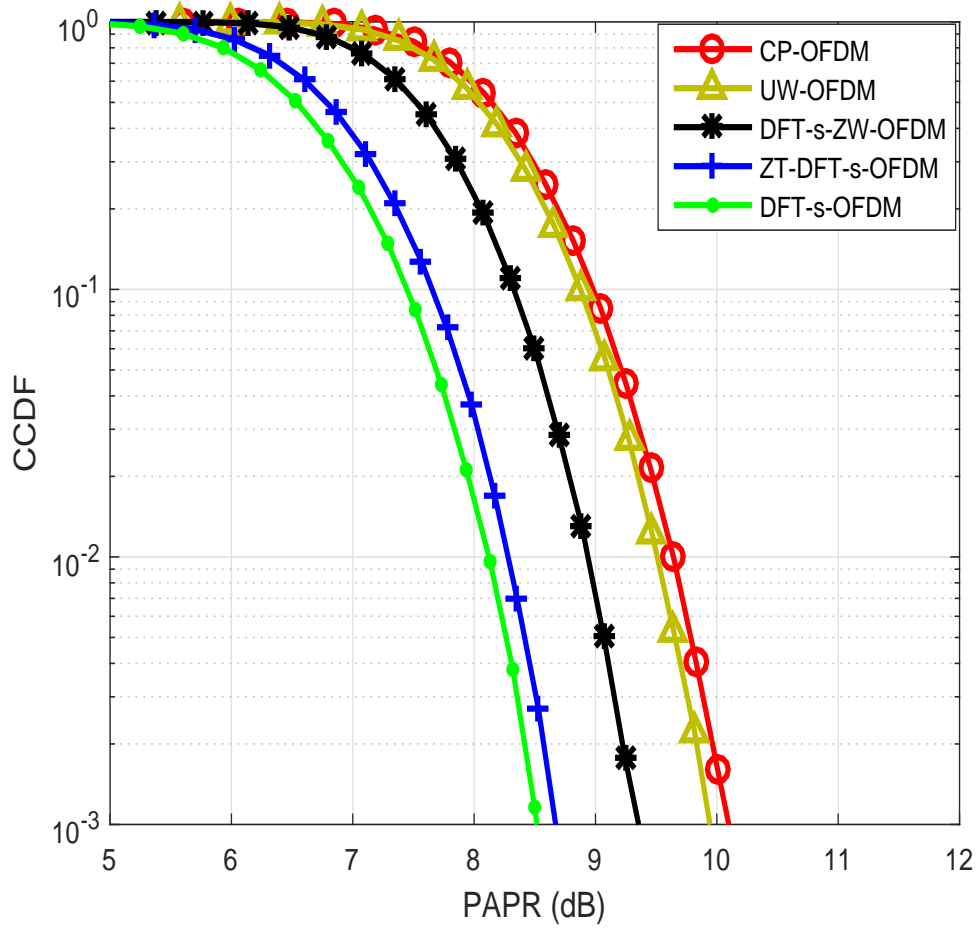


Fig. 2.3: PAPR comparison without considering tails.

Fig. 2.4 shows the power spectral density comparison and shows the superior performance of the DFT-s-ZW OFDM

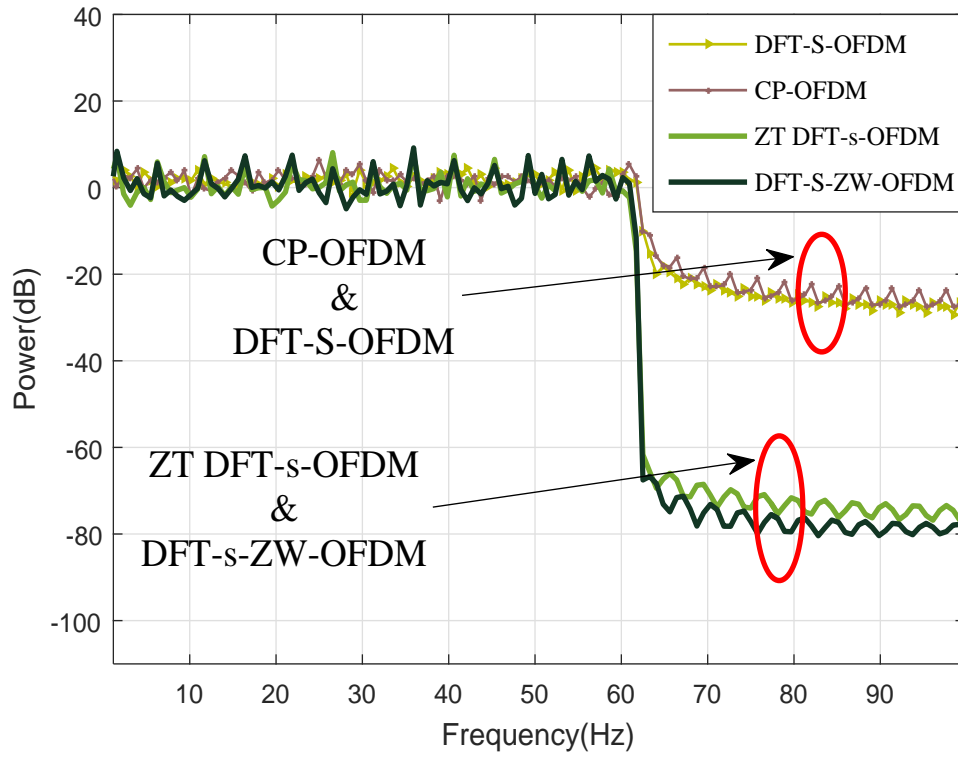
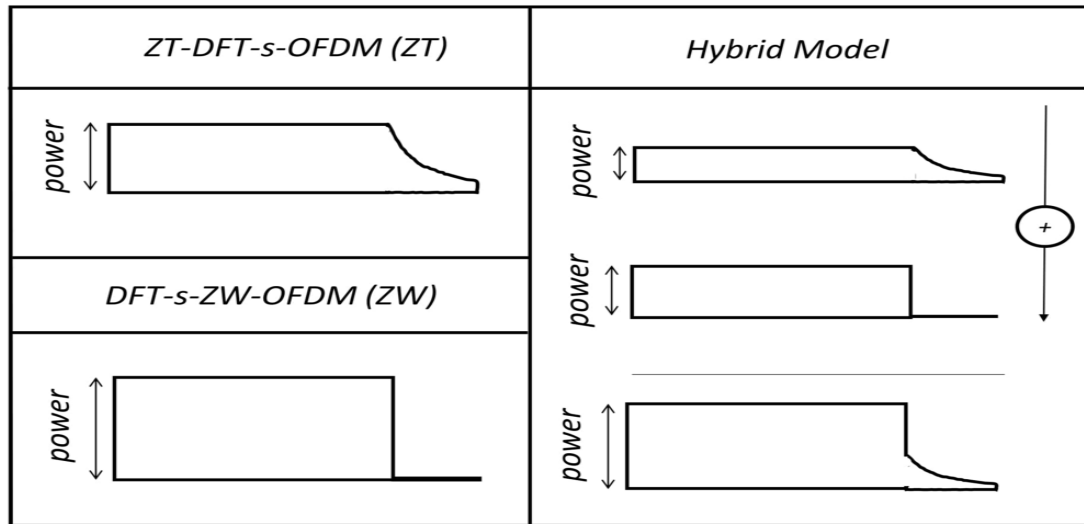


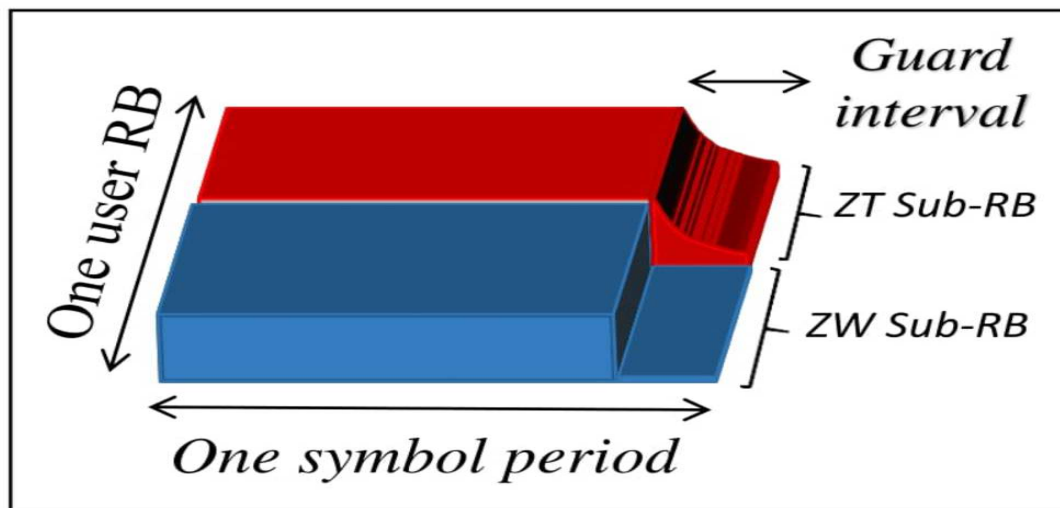
Fig. 2.4: Power spectral density comparison.

2.2 A Flexible Hybrid Waveform

Zero tail DFT spread OFDM (ZT DFT-s-OFDM) is one of the waveforms that has attracted lots of attention because of low OOB, lowPAPR and flexible guard intervals. However the non zero tail (despite of its name) cause ISI in the dispersive channels. DFT-s-ZT OFDM has zero tail thus there is no ISI at dispersive channel but due to redundant subcarriers it has higher PAPR in comparison to ZT DFT-s-OFDM. We propose a new waveform which can be either one of these waveforms or a combination of both.



(a) Comparison of symbol power and tail power in ZT-DFT-s-OFDM, DFT-s-ZW-OFDM and Hybrid model.



(b) Co-existence of two waveforms as two Sub-RBs with equal symbol periods and guard intervals.

Fig. 2.5: Proposed hybrid waveform.

Fig. 2.5 shows the proposed hybrid waveform. This hybrid model can be customized according to user requirement. In a situation that channel is highly dispersive more subcarriers can be assigned for DFT-s-ZW OFDM and less or none to ZT DFT-s-OFDM.

Fig. 2.6

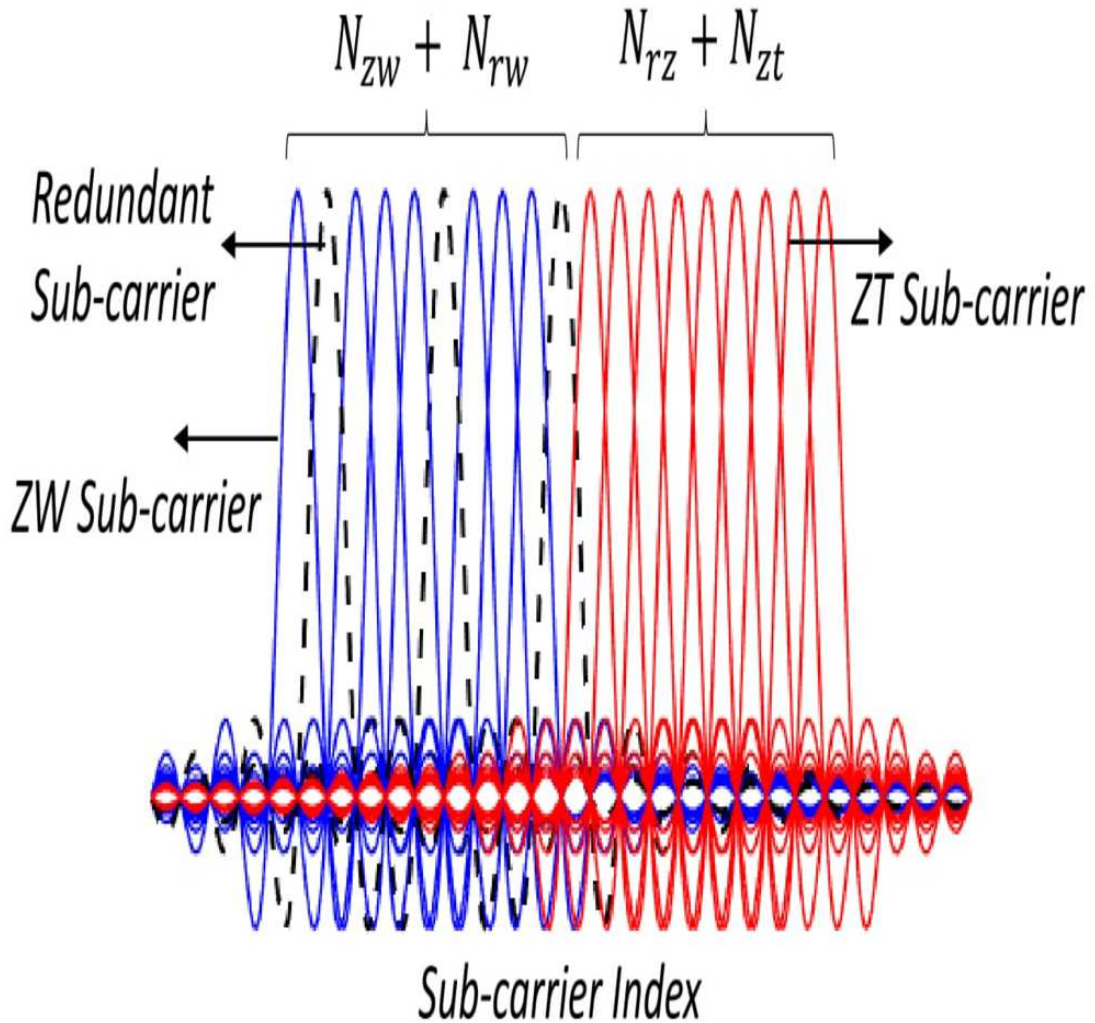
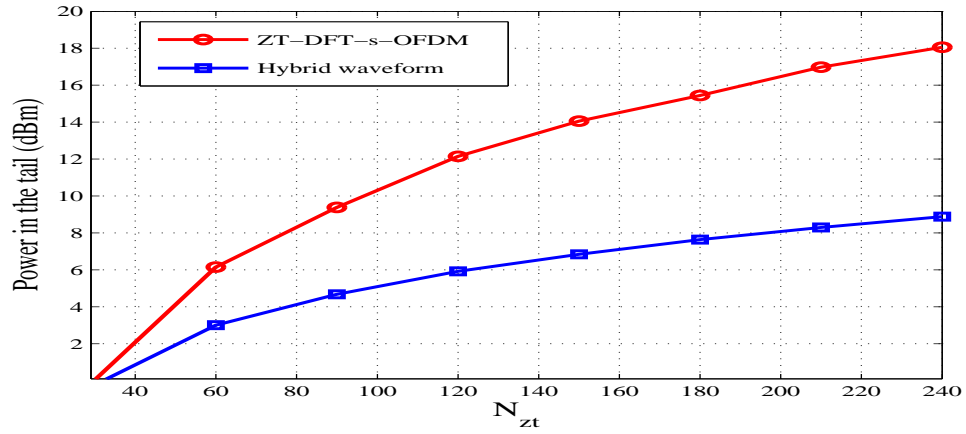
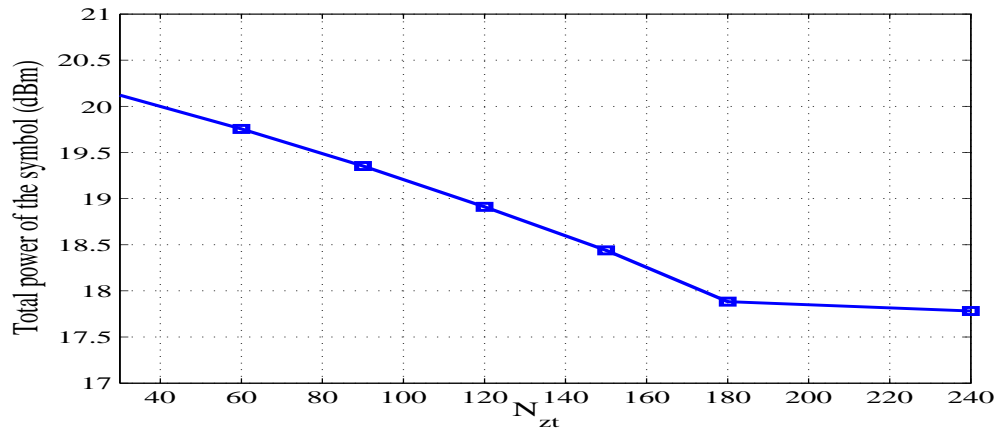


Fig. 2.6: Co-locating ZW and ZT subcarriers without a guard between them.

The trade-off between symbol power and tail power is shown in Fig. 2.7. The hybrid model has lower power tail than ZT DFT-s-OFDM due to use of DFT-s-ZW OFDM. The power of tail increases as the number of subcarriers assigned to ZT DFT-s-OFDM increases. However, the symbol power decreases as the number of subcarriers assigned to ZT DFT-s-OFDM increases due to use of less redundant subcarriers.



(a) Comparison of power in the tail of hybrid model and conventional ZT-DFT-s-OFDM. Tail power increases as N_{zt} increases.



(b) Symbol power of hybrid model is decreasing as N_{zw} increasing.

Fig. 2.7: Power evaluation. Trade-off between symbol power and tail power.

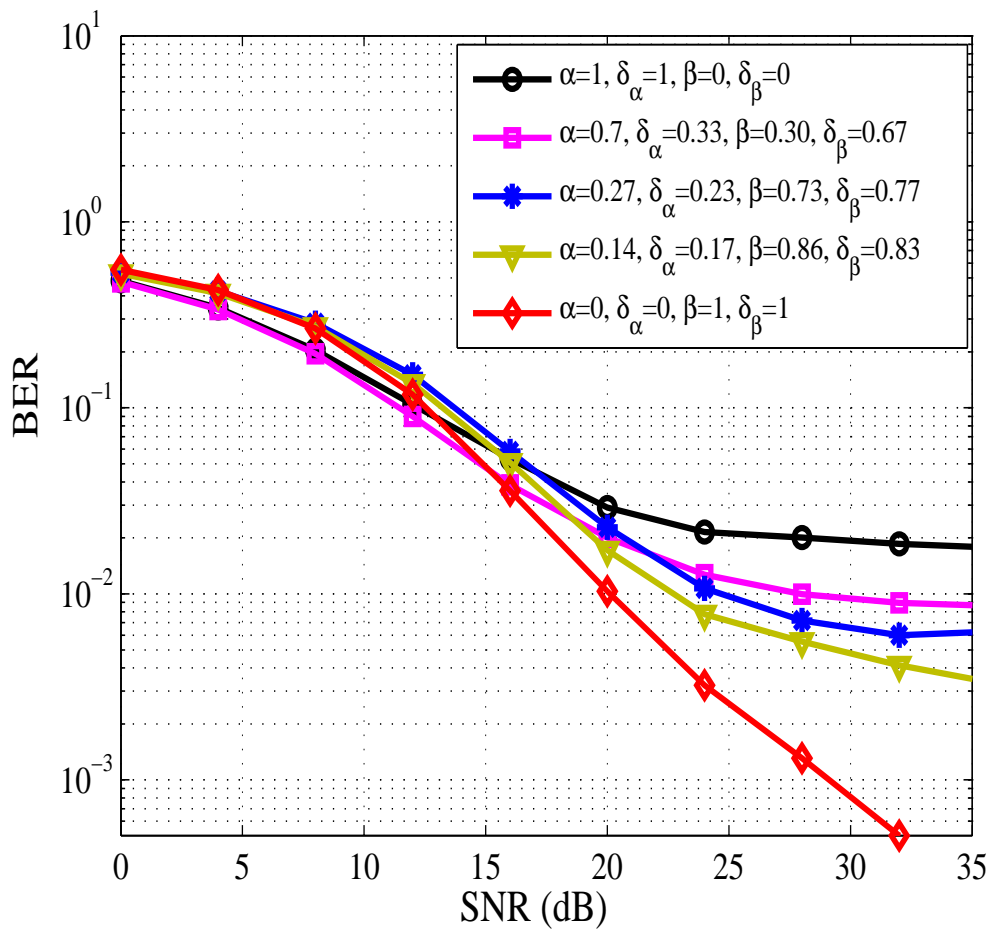


Fig. 2.8: BER performance of the hybrid waveform in Rayleigh fading channel with uniform PDP distribution, $\tau = 21$.

Fig. 2.8 shows the BER performance of hybrid waveform with different ratio of assigned subcarriers to ZT DFT-s-OFDM and DFT-s-ZW OFDM.

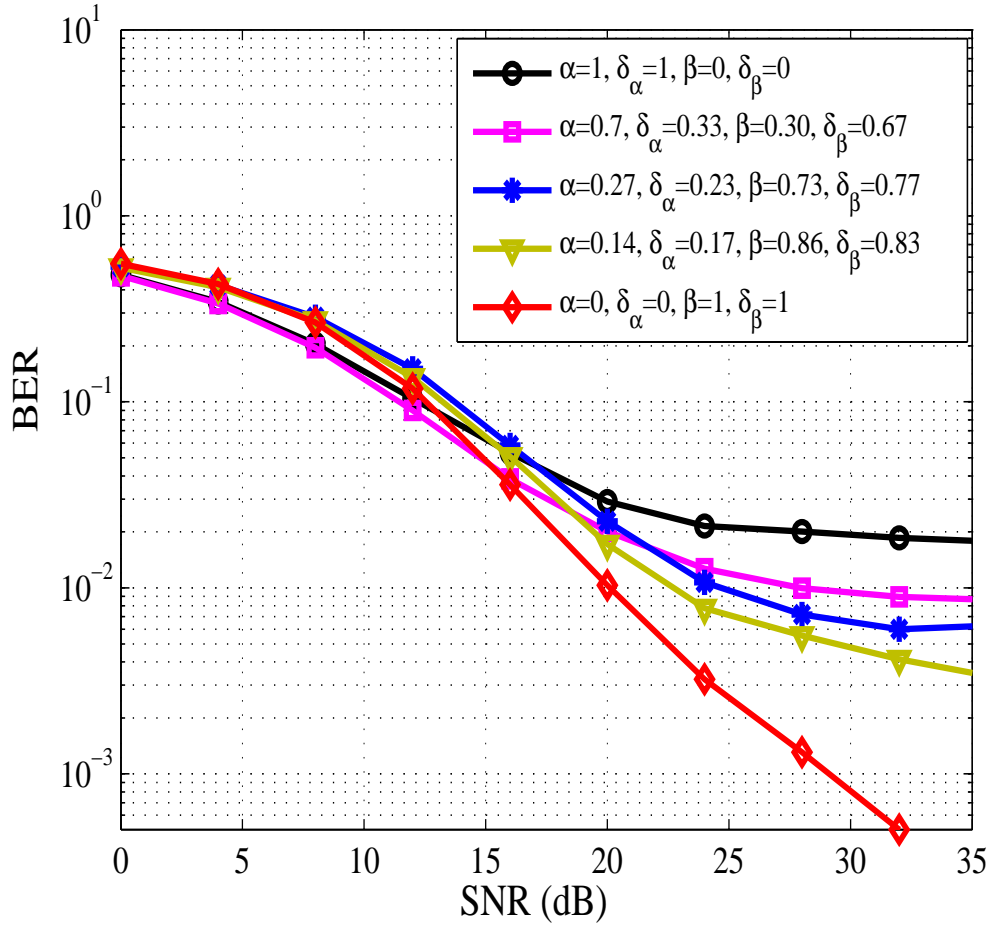


Fig. 2.9: Power spectral density comparison.

In Fig. 2.9 the power spectrum of hybrid waveform and CP-OFDM is shown. The superior performance of the hybrid waveform is demonstrated in Fig. 2.9.

Chapter 3

Joint Optimization of Device to Device Resource and Power Allocation based on Genetic Algorithm

3.1 System Model and Problem Formulation

A cellular cell with one base station in the center and a number of users are considered as shown in Figure ?? (a). The users are randomly distributed around the base station. Users are classified into two groups of cellular users and D2D users. Although the cellular users communicate through the base station, in D2D communication, a device communicates directly to another close by device. Two communicating devices form a D2D pair. The set of communications are defined as $\mathbf{N} = \{U_1, U_2, \dots, U_V, U_{V+1}, \dots, U_{V+K}\}$, where U_i shows the i^{th} communication. V and K are the total number of cellular users and D2D pairs, respectively. Therefore, the first V elements are cellular users and the next K elements are D2D pairs. In other words, the set of cellular users is denoted by $\mathbf{M} = \{U_1, U_2, \dots, U_V\}$

and the set of D2D pairs is defined by $\mathbf{D} = \{U_{V+1}, U_{V+2}, \dots, U_{V+K}\}$. The bandwidth is divided into narrow resource blocks. $\mathbf{R} = \{RB_1, RB_2, \dots, RB_Q\}$ indicates the set of the resource blocks. RB_i and Q denotes the i^{th} resource block and total number of resource blocks, respectively. Also, $\mathbf{A} = \{a_{i,r}\}$, $\mathbf{A} \in \{0, 1\}^{(V+K) \times Q}$ is resource assignment matrix. $a_{i,r} = 1$ means i^{th} user utilizes r^{th} resource block and $a_{i,r} = 0$ shows that the r^{th} resource block is not used by i^{th} user. It is also worth mentioning that since the downlink resources are almost fully occupied by high power transmitted signals from base station to the cellular users, the uplink resources of the cellular users are shared with D2D users in the proposed algorithm.

In Figure ?? (b), a directed graph based on the cell in Figure ?? (a) is created. The graph shows the interference between each pair of communications. Nodes in this graph represent a communication, either a cellular or a D2D communication. The edges are interference between two connected nodes. $\mathbf{I}_{i,j}$ is the edge weight which indicates the set of interference value from i^{th} node to j^{th} node at different resource blocks which is defined as:

$$\mathbf{I}_{i,j} = \{I_{i,j,1}, I_{i,j,2}, \dots, I_{i,j,Q}\}, \quad (3.1)$$

where $I_{i,j,r}$ is the interference from i^{th} node to j^{th} node at r^{th} resource block. It is worth mentioning the dashed line between U_1 and U_2 shows that sharing a resource block between two cellular users is not allowed. Since their receiver is the base station, if they share a resource block the receiver cannot differentiate the signals. Thus, there is no interference between cellular users.

Maximum spectral efficiency of i^{th} communication at r^{th} resource block, either cellular user or D2D pair, is denoted by $Se_{i,r}$ and defined based on Shannon formula as

$$Se_{i,r} = \log_2(1 + SINR_{i,r}), \quad (3.2)$$

where $SINR_{i,r}$ is the signal to interference plus noise ratio. The $SINR_{i,r}$ in (3.2)

is expressed as

$$SINR_{i,r} = \frac{a_{i,r}p_{i,r}g_{i,i,r}}{\sigma^2 + I_i^r}. \quad (3.3)$$

In (3.3), $p_{i,r}$ is the transmission power of the i^{th} node at r^{th} resource block and $g_{i,j,r}$ is the channel gain between transmitter of the i^{th} node and receiver of the j^{th} node at r^{th} resource block. σ^2 denotes the noise power. I_i^r is the total interference from other nodes to i^{th} node which can be written as

$$I_i^r = \sum_{j=1, j \neq i}^{V+K} a_{j,r} I_{j,i,r} = \sum_{j=1, j \neq i}^{V+K} a_{j,r} p_{j,r} g_{j,i,r}. \quad (3.4)$$

By substituting (3.4) in (3.3), we obtain

$$SINR_{i,r} = \frac{a_{i,r}p_{i,r}g_{i,i,r}}{\sigma^2 + \sum_{j=1, j \neq i}^{V+K} a_{j,r}p_{j,r}g_{j,i,r}}. \quad (3.5)$$

The goal is to maximize the spectral efficiency of the network, which can be written as

$$Se_{network} = \sum_{i=1}^{V+K} \sum_{r=1}^Q Se_{i,r} = \sum_{i=1}^{V+K} \sum_{r=1}^Q \log_2(1 + SINR_{i,r}). \quad (3.6)$$

As (3.6) shows, $Se_{network}$ depends on $SINR_{i,r}$. Moreover, as shown in (3.5), in addition to resource allocation which determines the interfering users, transmission power of the users determines the amount of the interference and affects the $SINR$ and consequently the spectral efficiency. Therefore, optimizing the transmission power of the users helps maximizing the spectral efficiency of the network and managing the interference. It is also evident that both cellular users and D2D users, have an upper limit for their transmission power. Cellular users also should meet a minimum $SINR$ to prevent a severe reduction in spectral efficiency while sharing their resource block. Thus, maximization problem can be formulated as follows

$$\begin{aligned}
\mathfrak{S} &= \arg \max_{p,a} \sum_{i=1}^{V+K} \sum_{r=1}^Q \log_2(1 + SINR_{i,r}) \\
&= \arg \max_{p,a} \sum_{i=1}^{V+K} \sum_{r=1}^Q \log_2 \left(1 + \frac{a_{i,r} p_{i,r} g_{i,i,r}}{\sigma^2 + \sum_{j=1, j \neq i}^{V+K} a_{j,r} p_{j,r} g_{j,i,r}} \right) \quad (3.7)
\end{aligned}$$

$$\text{subject to } \begin{cases} C_1 : \sum_{i=1}^V a_{i,r} \leq 1, & i \in \mathbf{M}, \forall r \in \mathbf{R} \\ C_2 : p_i < p_{d,max}, & i \in \mathbf{D} \\ C_3 : p_i < p_{c,max}, & i \in \mathbf{M} \\ C_4 : SINR_{i,r} \geq SINR_{min}, & i \in \mathbf{M}, \forall r \in \mathbf{R} \end{cases} \quad (3.8)$$

where C_1 shows that there is at most one cellular user in each resource block. C_2 and C_3 limit the power of the users to their upper limits. $p_{d,max}$, $p_{c,max}$ are maximum transmission power of D2D users and cellular users, respectively. C_4 shows that $SINR_{min}$ is minimum $SINR$ for the cellular users. It is worth mentioning that there is no restriction in the number of D2D users in one resource block as long as C_4 is met.

Finding a solution for an optimization problem with more than one constraint, similar to (3.7), is not possibly practical. Exhaustive search also is not applicable in engineering implementations due to the huge size of the search space. Therefore, to solve the constrained optimization problems, Genetic algorithm is a well known method [11]. In the next section, a new Genetic algorithm-based method is proposed to solve the multi-constrained problem in (3.7).

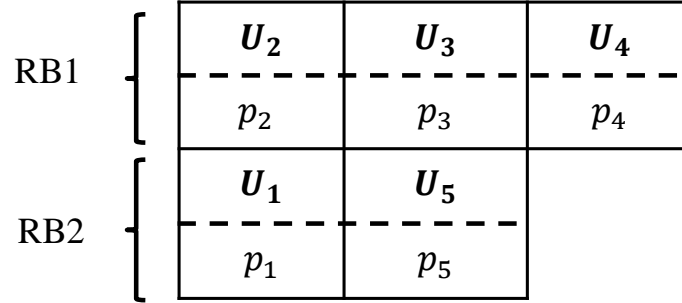


Fig. 3.1: A sample chromosome representation: RB_1 is shared by U_2 , U_3 and U_4 with power of p_2 , p_3 and p_4 , respectively. Also RB_2 is shared by U_1 and U_5 with power of p_1 and p_5 , respectively. $\mathbf{M} = \{U_1, U_2\}$ and $\mathbf{D} = \{U_3, U_4, U_5\}$ are cellular users and D2D pairs, respectively.

3.2 Algorithm Description

Genetic Algorithm emulates the process of natural selection. The algorithm starts with a set of candidate solutions (chromosomes). A chromosome presents dedicated powers and resource blocks to communications. Figure. 3.1 shows a sample chromosome, where two resource blocks are dedicated to five communications ($V = 2$ and $K = 3$), each with a specific transmission power. Additionally, each chromosome should satisfy the constraints of the optimization problem in (3.7). The set of chromosomes is called a generation. The generations are changed iteratively. At each iteration, chromosomes of the current generation are chosen to be parents and produce the children (offspring) for the next generation. The fitter chromosome, in terms of spectral efficiency, has higher chance to be selected as a parent. After series of iterations, the generation evolves toward the optimal chromosome. Moreover, the algorithm works with three operators to form a new generation based on the current generation: 1) *proportional selection*, 2) *crossover*, 3) *mutation*.

In the following, first, a metric for the fitness of a chromosome is given. Then, the operators based on the problem in (3.7) are defined.

3.2.1 Determining fitness function and power assignment

3.2.1.1 Fitness function

Fitness function measures the fitness of a chromosome. Since the purpose of the algorithm is maximizing spectral efficiency of the network, the fitness value of a chromosome equals to spectral efficiency of the network with respect to the chromosome. Therefore, fitness value of a chromosome can be written as

$$f_{\text{chromosome}} = \sum_{i=1}^{V+K} \sum_{r=1}^Q \log_2 \left(1 + \frac{a_{i,r} p_{i,r} g_{i,i,r}}{\sigma^2 + \sum_{j=1, j \neq i}^{V+K} a_{j,r} p_{j,r} g_{j,i,r}} \right). \quad (3.9)$$

3.2.1.2 Power assignment

Power of the users is also optimized during calculating fitness value. For this purpose, at each iteration, one D2D communication in each resource block (if there is any) is selected randomly. Power of the selected communication is optimized to maximize spectral efficiency of the desired resource block. Furthermore, the $SINR$ of the cellular user of the resource block (if there is any) is set to $SINR_{min}$ in order to serve more D2D users. Then, the power of i^{th} cellular user at r^{th} resource block is assigned based on (3.5) as

$$ip_{i,r} = SINR_{min} \times \frac{(\sigma^2 + \sum_{j=1, j \neq i}^{V+K} a_{j,r} p_{j,r} g_{j,i,r})}{a_{i,r} g_{i,i,r}}. \quad (3.10)$$

Additionally, if a resource block is used by only one communication, the transmission power of the communication is set to its maximum value. Algorithm 1 shows the pseudocode for fitness calculation and power assignment. Inputs to the algorithm are a chromosome (resource allocation matrix and transmission power vector). Also, the outputs are fitness value of the chromosome and optimized transmission power vector.

Next, we focus on mentioned operators and show that how they fit in the framework of our proposed method.

3.2.2 Proportional selection

Proportional selection operator selects the chromosomes based on their selection probabilities to be parents of next generation. The selection probability of a chromosome is based on its fitness value and can be expressed as

$$pr_s(x, t) = \frac{f_{\text{chromosome}}(x)}{\max(\text{fit}(t))}, \quad (3.11)$$

where x is a chromosome and $pr_s(x, t)$ is the probability of selecting x at t^{th} generation as a parent. $f_{\text{chromosome}}(x)$ is the fitness value of the chromosome x . Additionally, $\text{fit}(t)$ is the set of fitness values at t^{th} generation as

$$\text{fit}(t) = \{f_{\text{chromosome}}(x_1), f_{\text{chromosome}}(x_2), \dots, f_{\text{chromosome}}(x_{N_t})\} \quad (3.12)$$

where x_i and N_t are i^{th} chromosome and the total number of chromosomes in t^{th} generation, respectively.

3.2.3 Crossover operation

Crossover operator combines two parents and produces offspring for the next generation. At the beginning, a random length is dedicated to each resource block of the offspring where the sum of the lengths must be equal to total number of communications. This length shows the number of potential communications that can be supported in the intended resource block. Also, a random number in the range of $[1, V + K]$ is selected which is called *crossover point*. It determines the number of communications which are taken from each parent (e.g *crossover point* = 3 means three communications and their transmission powers are taken from parent 1 and the others are taken from parent 2). Figure 3.2 shows an example of

crossover operation, where p_{i-j} shows the transmission power of i^{th} user of j^{th} parent. In the figure, $\mathbf{M} = \{U_1, U_2\}$, $\mathbf{D} = \{U_3, U_4, U_5\}$ and lengths of resource blocks in the offspring are randomly selected to be 4 and 1, respectively. Also, the *crossover point* equals to 2. Therefore, first U_2 and U_4 are chosen from parent 1 and as the results of first and second moves, the two communications are set as the first two communications of the first resource block of the offspring. Other communications of offspring are taken from the second parent. First element of second parent is U_1 , but it cannot be set as the third communication of the offspring. The reason is that there is another cellular user (U_2) at the first resource block. Thus, in the third move, U_1 is added to the stack. As fourth move, U_5 is added to the offspring as the third communication. Since U_4 and U_2 already exist in the offspring, they are not added again. The last element in second parent is U_3 which as fifth move will be set as fourth communication of the offspring. The communications of the first resource block of the offspring is completed. The next communication is at the second resource block. Although there is no remaining elements in parent 2, the stack has one element. Thus, in the sixth and the last move, the element in the stack will be the only communication of the second resource block of the offspring. Moves are shown by numbers in the Figure 3.2. The pseudocode of crossover operation is given in Algorithm 2. Two chromosomes (parents) are the inputs to the algorithm and produced offspring is the output.

3.2.4 Mutation

In order to escape from local optimum solutions, the genetic algorithm adds a random change to chromosomes with a low probability [11]. For applying a random change in a chromosome, two users are selected randomly and swapped. In order to follow the first constraint in (3.8) (C_1), if the first selected user is among the D2D pairs (cellular users), the second one should also be selected among the D2D pairs (cellular users). Note that the probability of the mutation should be low to prevent a random search.

Combination of proportional selection, crossover operation and mutation is called select and reproduce. The pseudocode of select and reproduce function is given in Algorithm 3.

3.2.5 Optimization using genetic algorithm operators

The optimization algorithm, as shown in Algorithm 4, starts with a random generation. Random generation generate N_t random chromosomes as the first generation. Power of the users is set to their upper limit in the beginning. Then, fitness value of all the chromosomes in the generation is calculated. Next, the select and reproduce function is called. In the function, parents are selected according to their fitness value and then, offspring are produced. Mutation is also applied on the offspring at this step. Therefore, generation is updated and algorithm is repeated *rep* times. Tuning the mutation rate and crossover rate is usually done by means of trail-and-error [24].

In order to assign the resource blocks and transmission power of users efficiently, having the prior knowledge of interference between the users is required. In other words, CSI is required to be known prior to the resource and power allocation. In the following section, we describe a channel prediction algorithm which results in a lower transmission overhead.

3.3 Channel prediction

Performance of adaptive communication systems depends heavily on knowledge of CSI. Interference aware resource allocation is also an adaptive system. Knowledge of the CSI in adaptive systems, is usually provided through feedback. After establishing a connection between the intended users, the receiver estimates the channel and then, feeds it back either to the transmitter or the base station. This

process does not only result in a huge load on the network, but also the fed back information can be outdated due to delay caused by the feedback. An error in CSI or an outdated information results in a wrong decision in the system. Thus, instead of feeding back the CSI from each user or using outdated CSI by periodically collecting CSI, a prediction method at the base station for CSI is used [3, 14, 15, 42, 18, 16].

In our system model, we assume a flat fading channel. The reason lies in dividing the bandwidth into small and narrow bands. Therefore, users experience a flat fading channel. Taps of a channel act as sum of the sinusoids [17]. This sum of sinusoids can be modeled as an autoregressive (AR) process. Let y_t denote the received data at the t^{th} time. h_t is the complex quantity of time-based channel impulse at t^{th} time instance and b_t is the transmitted modulated data (e.g. BPSK). y_t can be defined as:

$$y_t = h_t b_t + z_t, \quad (3.13)$$

where z_t is the Added White Gaussian Noise (AWGN). Then, predicting the $(n + 1)^{\text{th}}$ sample based on the previous L samples can be done using a linear prediction.

$$h_{n+1} = \sum_{i=1}^L w_i h_{n+1-i}, \quad (3.14)$$

where the w is the predictor coefficient and is calculated as

$$w = R^{-1}r \quad (3.15)$$

where R is the autocorrelation matrix with coefficient $R_{ij} = \mathbf{E}[h_{n-i}h_{n-j}^*]$ and r is the autocorrelation vector with coefficient $r_j = \mathbf{E}[h_n h_{n-j}^*]$ [16].

In the next section, the performance of the algorithm is evaluated using numerical simulations.

Table 3.1: System Numerical Parameters

System Parameters	Corresponding value
Cell radius	500 m
Channel model	Winner model
Carrier frequency	1.8 GHz
Bandwidth of resource blocks	180 KHz
Number of resource blocks	8
Number of cellular users	4
Maximum distance between D2D pairs	10 m
Maximum power of D2D transmitters	23 dBm
Maximum power of cellular users	23 dBm
Noise power density	-174 dBm
Number of repetition in genetic algorithm	50

3.4 Simulation Results

In this section, the performance of the algorithm under different scenarios is evaluated. The evaluations include: A) network spectral efficiency evaluation, B) cumulative distribution function (CDF) comparison, C) network interference power evaluation. In all the simulations, radius of the cell is assumed to be 500 m. There is a base station in the center of the cell. The users are distributed randomly around the base station. Maximum distance between D2D pairs is set to 10 m [12]. Carrier frequency, resource blocks bandwidth and maximum power of users (D2D transmitters and cellular users) are set as in long term evolution (LTE) to 1.8 GHz, 180 kHz and 23 dBm, respectively [55]. The parameters used in simulation results are given in Table 3.1, unless otherwise specified. Each user is assumed to have an omni-directional antenna. Without loss of generality for the case of simplicity, for all the scenarios, an indoor channel model according to Winner model is considered. In the case of outdoor, due to the significant difference in antenna height for base station and users (cellular and D2D users) two different channel models should be considered, one for cellular users and one for D2D users. The channel gain consists of large scale pathloss and small scale fading. Large scale pathloss, denoted by PL , based on Winner model is defined

[27] as

$$PL(dB) = 22.7 \log_{10} d + 27 + 20 \log_{10} f_c. \quad (3.16)$$

The small scale fading is assumed to be Rayleigh fading and is modeled by jakes model as

$$h_I(t) = 2 \sum_{n=1}^{N_0} (\cos \phi_n \cos w_n t) + \sqrt{2} \cos \phi_N \cos w_d t \quad (3.17)$$

and

$$h_Q(t) = 2 \sum_{n=1}^{N_0} (\sin \phi_n \cos w_n t) + \sqrt{2} \sin \phi_N \cos w_d t, \quad (3.18)$$

where $h_I(t)$, $h_Q(t)$, ϕ_n and ϕ_N are the real and imaginary components of channel at t^{th} time instance, initial phases of the n^{th} doppler shifted sinusoid and maximum doppler frequency (f_m) shifted sinusoid, respectively and $w_d = 2\pi f_m$ with $w_n = w_d \cos \phi_n$ [10]. The model is used to obtain L channel samples and the next samples are predicted using (3.14).

3.4.1 Network Spectral Efficiency Evaluation

This subsection is divided into three comparisons. The first is the comparison of the throughput of the proposed algorithm, GAAM[45], orthogonal[51], and random resource allocation. Figure 3.3 shows the outperformance of the proposed algorithm compared to GAAM, orthogonal, and random resource allocation. In this figure, $Q = 8$, $V = 4$ and K is varied from 2 to 18. In GAAM, a resource block is shared by a cellular user and a D2D pair. Thus, when Q equals to 8 at most 8 cellular users and 8 D2D pairs are served. Since $V = 4$, the maximum number of served communications is $4 + 8 = 12$. Thus, the curve for GAAM is increasing until number of communications equal to 12, and after that it is almost constant. In the orthogonal resource allocation, first, the 4 of 8 resource allocation is assigned to 4 cellular users. Then, the other resources are assigned to random D2D pairs. Therefore, after 8 number of communications, the slope of the curve decreases significantly. In the random and the proposed algorithm, as the number of communications increases, the spectral efficiency increases as well. The reason lies in having flexible number of D2D pairs in a resource block. It is

shown that even the random resource allocation can do better than GAAM and orthogonal resource allocation in dense and crowded environment.

The second comparison in this subsection evaluates the effect of number of resource blocks on the spectral efficiency. In Figure 3.4, the number of cellular users is fixed, $V = 8$ and K is varying from 7 to 152. It is shown that as the number of resource blocks - Q - increases, the spectral efficiency increases. The reason is that as more resource blocks results in less interference between the users. The difference in spectral efficiency for lower number of K is less than higher numbers of K due to the minimum $SINR$ that each cellular user should met. There is a trade-off between having better performance or lower number of resource blocks. Having more resource blocks leads to higher cost and better performance. The trade-off depends on the minimum expected spectral efficiency and number of communications expected to be served.

Third comparison is with respect to the repetition parameter of the genetic algorithm, denoted by rep . The parameter shows the number of produced generations. In Figure 3.5, spectral efficiency for different values of rep is shown. As rep gets larger, algorithm results in a better optimization. Higher number for repetition makes the algorithm finds a better solution but the algorithm needs to be run longer. Therefore, there is another trade-off between having higher performance or lower number for repetition. However, when rep is large enough, e.g. $rep = 50$, result of the algorithm is an acceptable solution and good enough. As the figure shows the curves for $rep = 50, 100, 200$ are very close.

3.4.2 CDF Evaluation

Figure 3.6 shows the CDF curves of the proposed algorithm, GAAM [45], orthogonal [51] and random resource allocations. In the simulations, Q, V and K are assumed to be 8, 4 and 8, respectively. The CDF curves shows the ranges of the output algorithms. As Figure 3.6 shows, the proposed algorithm outperforms the

other methods. It also shows that random resource allocation can even perform better than orthogonal resource allocation. Moreover, random resource allocation has the widest range.

3.4.3 Interference Evaluation

Figure 3.7 shows the amount of the intra-cell interference for the proposed algorithm with different repetitions. The parameters for this simulation is the same as Figure 3.5. It is shown that for higher number of repetition, There is less interference. In other words, at each iteration a better and more optimized solution is found. Considering Figures 3.5 and 3.7, the proposed algorithm results in higher spectral efficiency at each iteration by mitigating the interference.

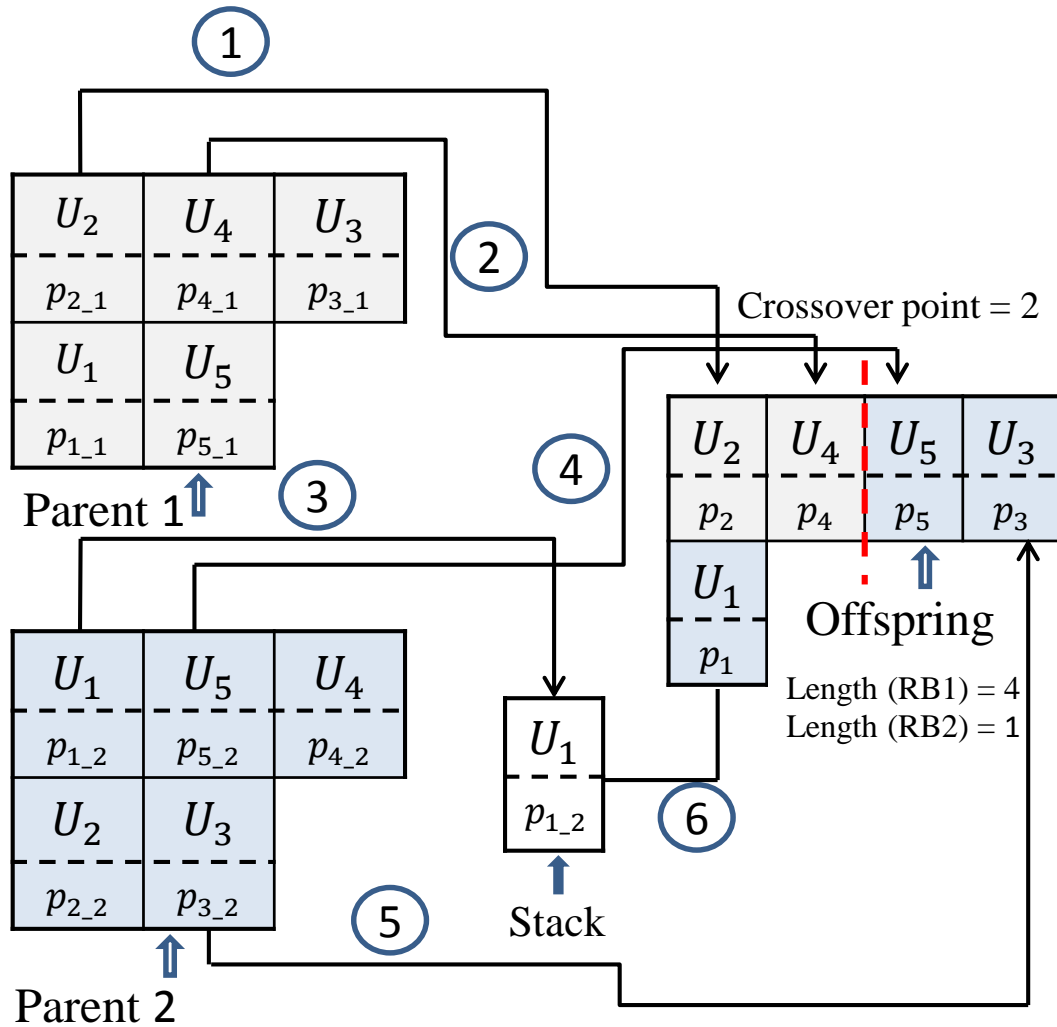


Fig. 3.2: Crossover operation. Parent 1 and Parent 2 produce offspring. crossover point randomly is selected and equals to 2. Moreover, length of two resource blocks, which are randomly selected, equal to 4 and 1, respectively.

Algorithm 1 Fitness Calculation and Power Assignment

```
1: procedure FIT_CALC (resourceVector, powerVector)
2:   Output fitness_value, powerVector
3:   Initialization: sum_vector =  $\emptyset$ ; cellVector =  $\emptyset$ ;
4:   for RB_member each row in resourceVector
5:     if there is any D2D pair in RB_member
6:       Select optd randomly among D2D pairs of
7:       RB_member
8:       for All possible values popt for power of optd
9:         temp  $\leftarrow$  powerVector
10:        Update temp with popt for optd
11:        if there is any cellular user in RB_member
12:          cell  $\leftarrow$  cellular user in RB_member
13:          p(cell)  $\leftarrow$  required power for SINRmin
14:          Add p(cell) to cellVector
15:          if p(cell)  $\leq$  pc,max
16:            Update temp with p(cell)
17:            rate  $\leftarrow$  sumrate of RB_member
18:            with respect to temp
19:          else
20:            rate  $\leftarrow$   $-\infty$ 
21:          end if
22:        else
23:          rate  $\leftarrow$  sumrate of RB_member with
24:          respect to temp
25:        end if
26:        Add rate to sumVector
27:      end for
28:      sumrate(RB_member)  $\leftarrow$  max(sumVector)
29:    else
30:      p(cell)  $\leftarrow$  pc,max
31:      Update powerVector with p(cell)
32:      sumrate(RB_member)  $\leftarrow$  sumrate of
33:      RB_member with respect to powerVector
34:    end if
35:  end for
36:  fitness_value  $\leftarrow$  sum(sumrate)
```

Algorithm 2 Crossover

```
1: procedure CROSSOVER (Parent1, Parent2)
2:   Output offspring
3:   Initialization:  $i = 1$  and  $done = 0$ 
4:   select  $Len = \{len(1), len(2), \dots, len(Q)\}$  randomly in a way that  $len(1) + len(2) + \dots + len(Q) = V + K$ 
5:    $crossover\_point \leftarrow$  random number 1 to  $V + K$ .
6:   for  $rb = 1$  to  $Q$ 
7:     while  $done = 0$ 
8:       if  $i \leq crossover\_point$ 
9:          $temp \leftarrow i^{th}$  communication of the Parent1.
10:      else
11:         $temp \leftarrow (i - crossover\_point)^{th}$  communication of the Parent2.
12:        while  $temp$  is already taken from Parent1
13:           $i \leftarrow i + 1$ 
14:           $temp \leftarrow (i - crossover\_point)^{th}$  communication of the Parent2.
15:        end while
16:        for  $pos = 1$  to  $len(rb)$ 
17:          If  $pos$  is for a D2D pair and  $temp$  is a D2D pair
18:             $offspring(rb, pos) \leftarrow temp$ 
19:             $i \leftarrow i + 1$ 
20:             $done = 1$ 
21:          else if  $pos$  is for a D2D pair and  $temp$  is a cellular user
22:            Add  $temp$  to the Cell_Stack
23:             $i \leftarrow i + 1$ 
24:          else if  $pos$  is for a cellular user and  $temp$  is a cellular user
25:             $offspring(rb, pos) \leftarrow temp$ 
26:             $i \leftarrow i + 1$ 
27:             $done = 1$ 
28:          else if  $pos$  is for a cellular user and  $temp$  is a D2D pair
29:            if Cell_Stack is not empty
30:               $offspring(rb, pos) \leftarrow Cell\_Stack(1)$ 
31:              Delete the first element in Cell_Stack.
32:               $done = 1$ 
33:            else
34:               $offspring(rb, pos) \leftarrow 0$ 
35:               $done = 1$ 
36:            end if
37:          end if
38:        end for
39:      end while
40:    end for
```

Algorithm 3 Select and Reproduce

```
1: procedure SEL_REP (gen, fit)
2:   Output new_gen
3:   max_fit  $\leftarrow$  max(fit)
4:   for each chromosome in gen
5:      $pr_s(\text{chromosome}) = \frac{\text{fit}(\text{chromosome})}{\text{max\_fit}}$ 
6:   end for
7:   for chr = 1 to  $N_t$ 
8:     p1, p2  $\leftarrow$  choose two parents based on the probability
9:     new_in  $\leftarrow$  Crossover(p1, p2)
10:    mut  $\leftarrow$  random number 0 to 1
11:    if mut  $\leq$  0.2
12:      mut_gen  $\leftarrow$  Choose two cellular users or two
13:      D2D pairs and swap them
14:      Add mut_gen to new_gen
15:    else
16:      Add new_in to new_gen
17:    end if
18:  end for
```

Algorithm 4 Optimization

```
1: procedure OPTIMIZATION (rep)
2:   Output best_individual
3:   Initialization: ;
4:   (initial_generation)  $\leftarrow$  random generation
5:   i  $\leftarrow$  1
6:   do:
7:     fit =  $\emptyset$ 
8:     for each chr in next_gen:
9:       (fit_chr, Power)  $\leftarrow$ 
10:      Fit_Calc(chr.resourceVector, chr.powerVector)
11:      chr.powerVector  $\leftarrow$  Power
12:      Add fit_chr to fit
13:    end for
14:    next gen  $\leftarrow$  Sel_Rep(fit, next_gen)
15:    i  $\leftarrow$  i + 1.
16:  while i < rep
17:  best_individual  $\leftarrow$  max(fit)
18:
```

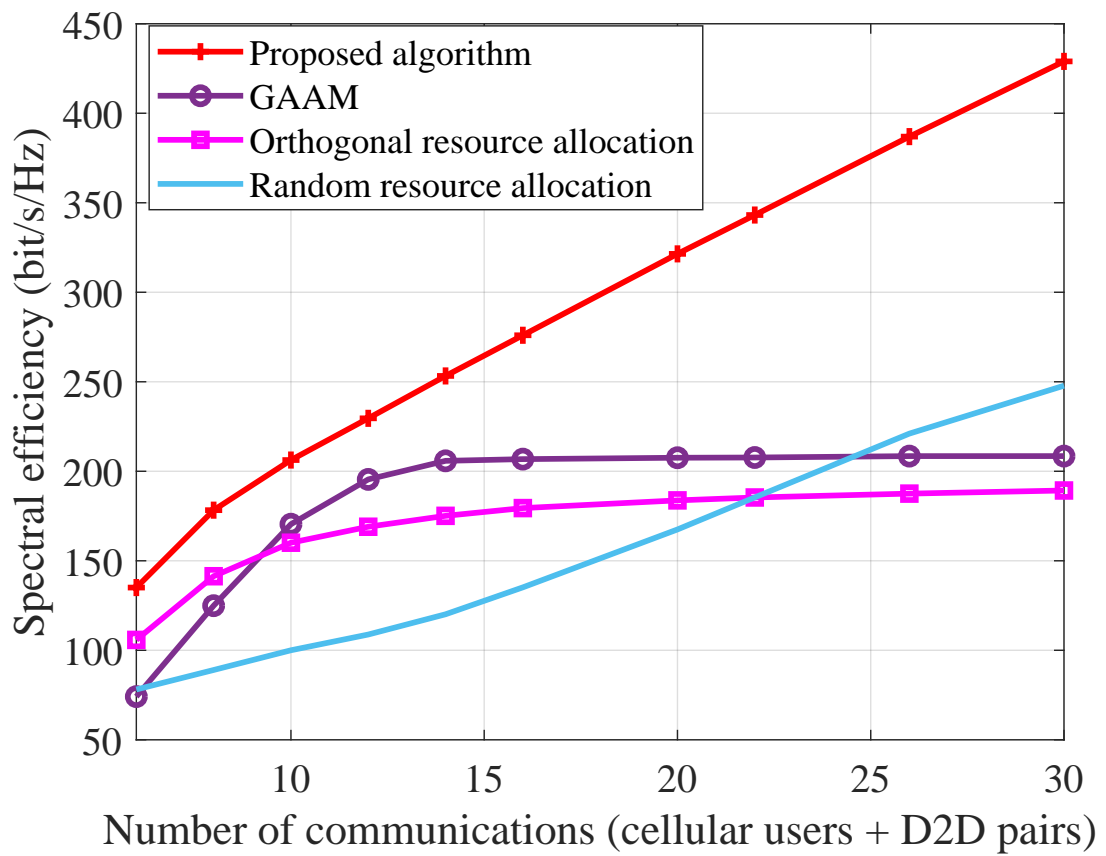


Fig. 3.3: Spectral efficiency for different number of resource blocks.

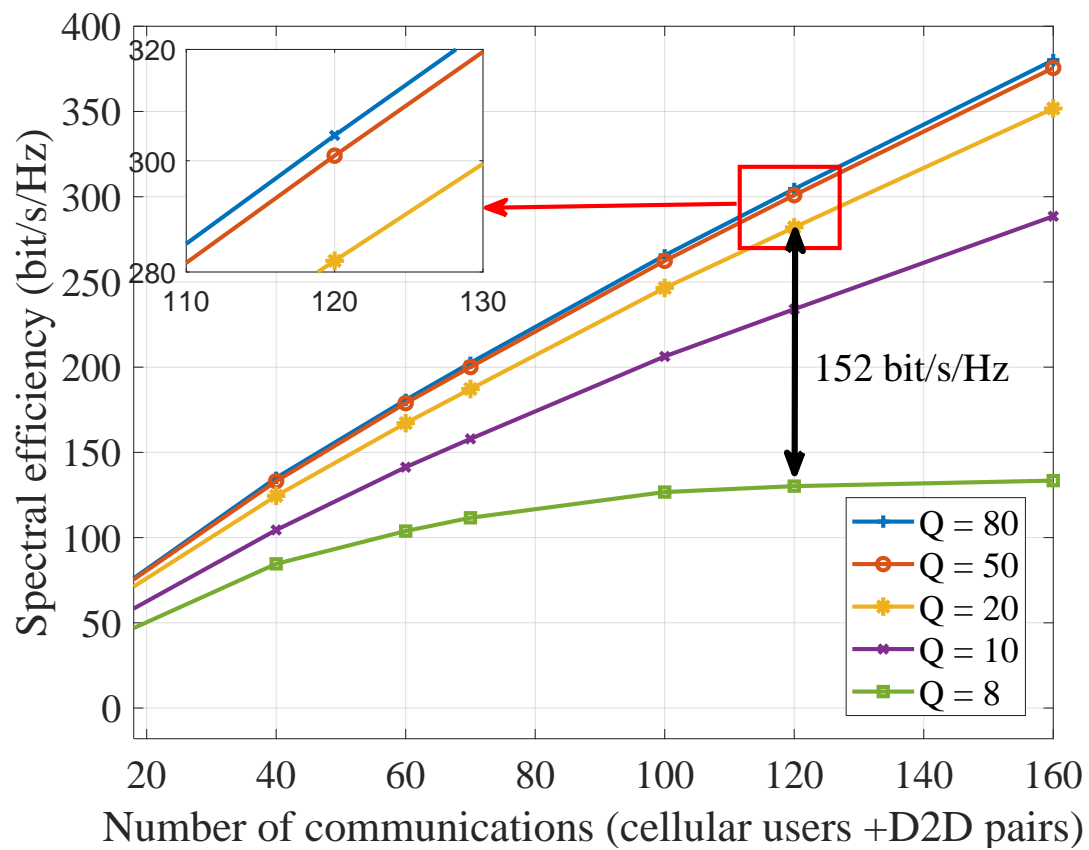


Fig. 3.4: Spectral efficiency with respect to the number of available resource blocks.

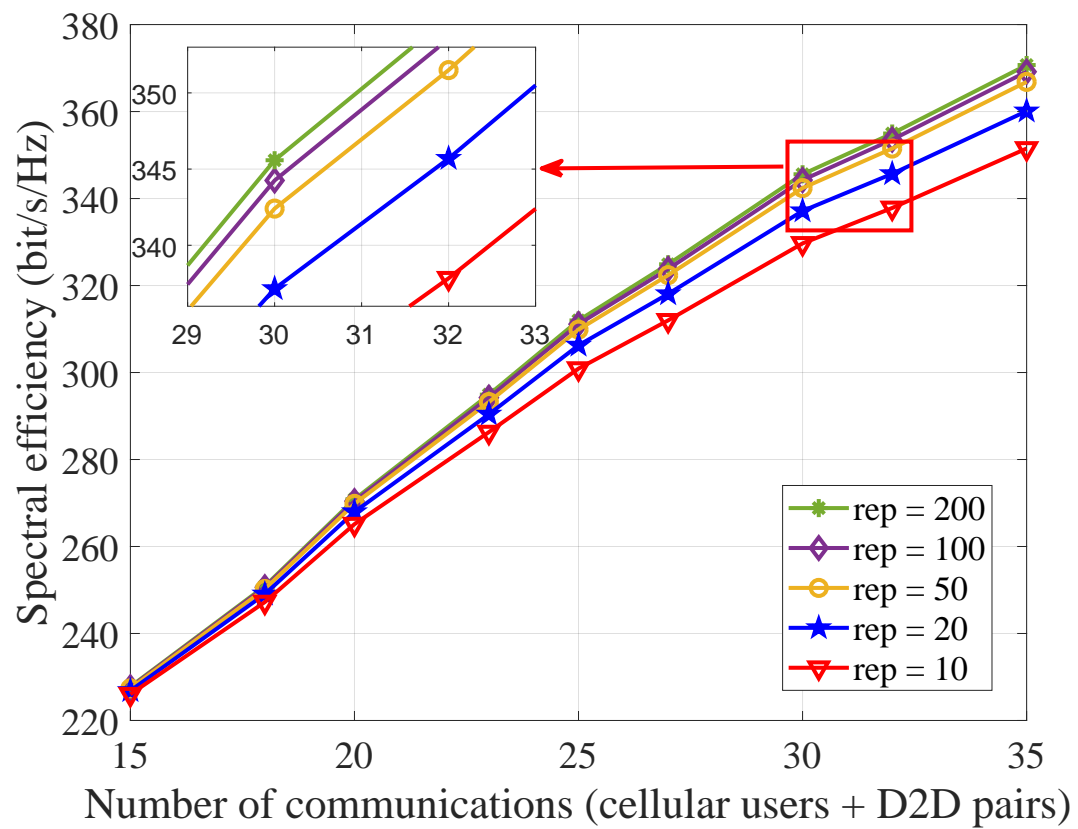


Fig. 3.5: Spectral efficiency for different number of repetitions.

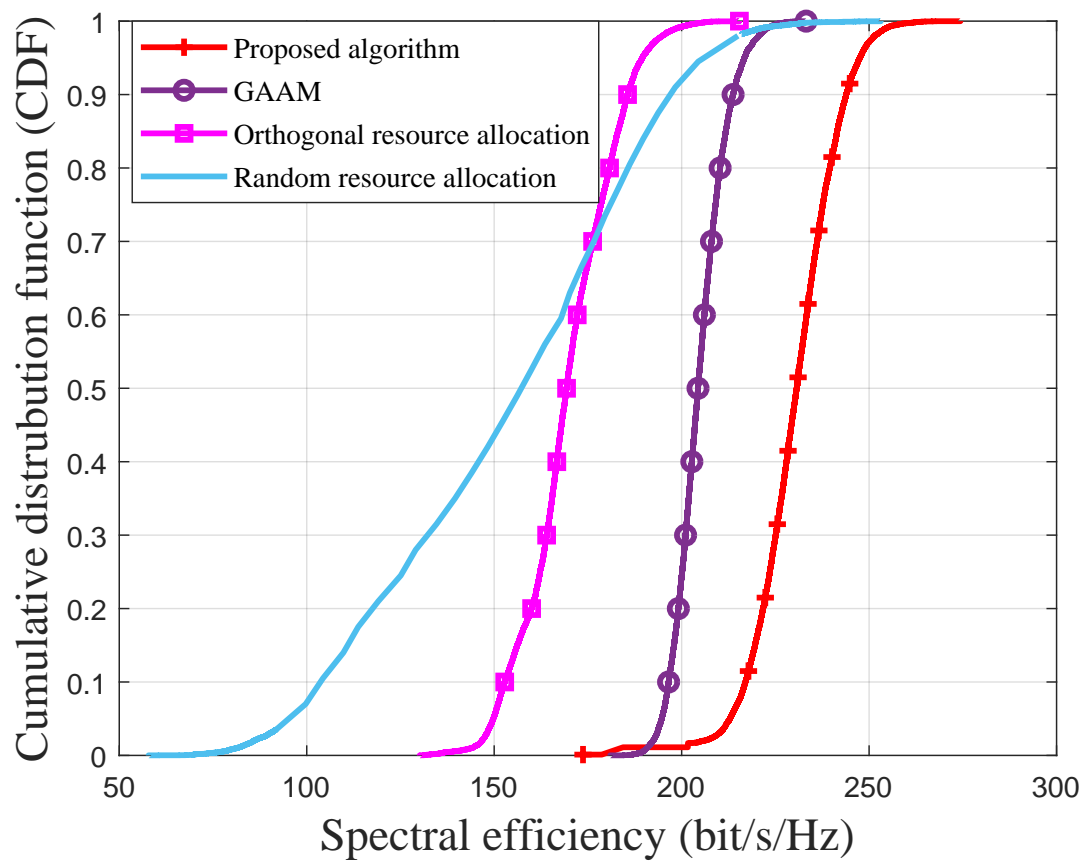


Fig. 3.6: Cumulative distribution function of spectral efficiency.

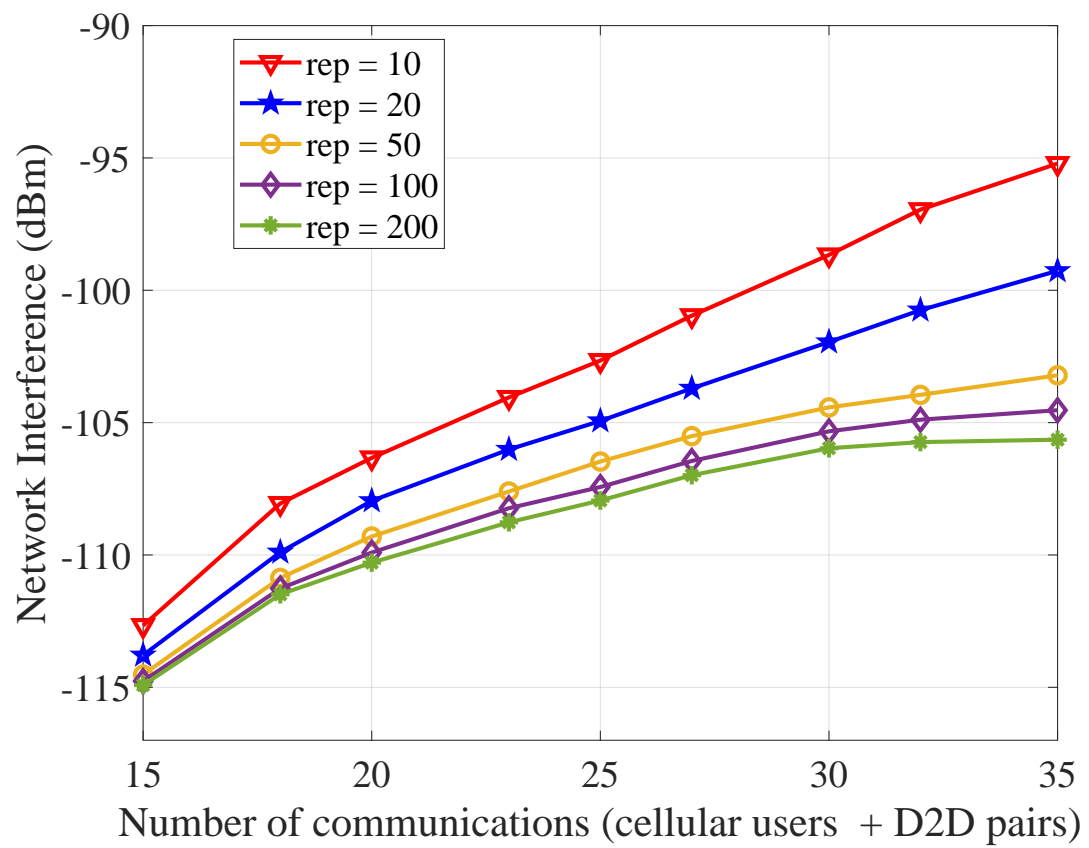


Fig. 3.7: Network interference for different number of repetitions.

Chapter 4

A Novel One-Base Station Hybrid Positioning Method

4.1 System Description

The PuOB method utilizes AOA and TDOA positioning methods in order to achieve a highly reliable and low cost hybrid positioning estimation and tracking method.

The first and second parts of the system description is dedicated to TDOA and AOA equations used in this work. The third part describes the PuOB method.

Notation: M and N are the total number of assumed BSs in an arbitrary positioning method and total number of time instances that the measurements are taken, respectively. $\|\cdot\|$ and $(\cdot)^T$ denote the L^2 -norm operation and the transpose operation of a matrix, respectively. Let c denote the velocity of the transmitted signal.

4.1.1 Time Difference of Arrival (TDOA) Method

The conventional TDOA method uses the time of arrival differences between a received signal at different BSs. As shown in Fig. 1, each BS acts as a focus of a hyperbola in conventional TDOA method. The intersection of these hyperbolas provides the estimated location of the transmitter.

Let \mathbf{S}_m denote m^{th} BS located at $[x_m, y_m, z_m]^T \in \mathbb{R}^3$ in Cartesian coordinates where $m = 1, 2, \dots, M$. The coordinates of the mobile transmitter at the time of t_n , $n = 0, 1, \dots, N$ is defined as $\mathbf{P}_n = [x_n, y_n, z_n]^T \in \mathbb{R}^3$. Then, in the absence of measurement noise, distance $r_{m,n}$ between the transmitter at time instance of t_n and m^{th} BS can be modeled as

$$r_{m,n} = cT_{m,n} = \|\mathbf{P}_n - \mathbf{S}_m\| \quad (4.1)$$

$$= \sqrt{(x_n - x_m)^2 + (y_n - y_m)^2 + (z_n - z_m)^2}, \quad (4.2)$$

where $T_{m,n}$ is the duration for the signal to travel from the transmitter to the BS. By considering two BSs as foci of a hyperbola, the distance difference between the transmitter and the two BSs, m^{th} and $(m-1)^{\text{th}}$ BSs, can be given as $d_{(m,m-1),n} = c(T_{m,n} - T_{(m-1),n}) = r_{m,n} - r_{(m-1),n}$, where $d_{(m,m-1),n}$ is fixed-difference property that can be used for positioning on hyperbolas ($|r_{m,n} - r_{(m-1),n}| = d_{(m,m-1),n}$ for every point on the hyperbolas). As shown in Fig. 4.1, for a simple hyperbola, at least two BSs are required. In order to have a TDOA positioning estimation of a transmitter in 3-D coordinates, at least 3 hyperbolas produced by measurements at 4 BSs are necessary.

4.1.2 Angle of Arrival (AOA) Method

In this part, we extract the relations of AOA which is used in the PuOB method. \mathbf{S}_m is assumed to be in the origin of Cartesian coordinates, in $r_{n,m}$ distance of \mathbf{P}_n as given in (4.2). The unit vector from BS toward the transmitter is the resultant

of three vectors in each Cartesian axis,

$$\mathbf{P}_n - \mathbf{S}_m = r_{m,n} \begin{bmatrix} \cos \alpha_{m,n} & \cos \beta_{m,n} & \cos \gamma_{m,n} \end{bmatrix}^T, \quad (4.3)$$

where $\alpha_{m,n}$, $\beta_{m,n}$ and $\gamma_{m,n}$ are the angles of received signal with x, y, z axes. In order to measure the angles of arrival at each axis, similar to [32], we assume antenna arrays are used. As shown in Fig. 2, for measuring $\alpha_{m,n}$ which is the angle of received signal with x-axis at m^{th} BS, there is a simple antenna array in x-direction. So, $\alpha_{m,n}$ is defined as $\alpha_{m,n} = \cos^{-1} \left(\frac{c|t_2 - t_1|}{\ell} \right)$, where t_1 and t_2 are the time instances of received signal to antenna 1 and antenna 2, respectively. ℓ is the known distance between two antennas. $\beta_{m,n}$ and $\gamma_{m,n}$ can be found like $\alpha_{m,n}$ with a 3D antenna setup.

Equation (4.3) presents that the vector $\mathbf{P}_n - \mathbf{S}_m$ is equal to $r_{m,n}$ multiplied by the unit vector of $\mathbf{P}_n - \mathbf{S}_m$. Let $\mathbf{b}_{m,n}$ denote the unit vector,

$$\mathbf{P}_n - \mathbf{S}_m = r_{m,n} \mathbf{b}_{m,n}. \quad (4.4)$$

According to (4.3) and Fig. 3, $\mathbf{b}_{m,n}$ in Spherical coordinates is defined as:

$$\mathbf{b}_{m,n} = \begin{bmatrix} \sin \theta_{m,n} \cos \phi_{m,n} & \sin \theta_{m,n} \sin \phi_{m,n} & \cos \theta_{m,n} \end{bmatrix}^T \quad (4.5)$$

In (4.5), $\theta_{m,n} \in [0, \pi]$ and $\phi_{m,n} \in [0, 2\pi]$ are defined as

$$\mathbf{A}_{m,n} = \begin{bmatrix} \phi_{m,n} \\ \theta_{m,n} \end{bmatrix} = \begin{bmatrix} \tan^{-1} \left(\frac{\cos \beta_{m,n}}{\cos \alpha_{m,n}} \right) \\ \tan^{-1} \left(\frac{\sqrt{\cos^2 \alpha_{m,n} + \cos^2 \beta_{m,n}}}{\cos \gamma_{m,n}} \right) \end{bmatrix}, \quad (4.6)$$

where $\mathbf{A}_{m,n}$ denotes the AOA measurements matrix.

4.1.3 Positioning using One Base Station (PuOB) Method

Fig. 3 depicts how a BS and position of a transmitter in two time instances can be used by the PuOB method. The transmitter in two time instances plays the

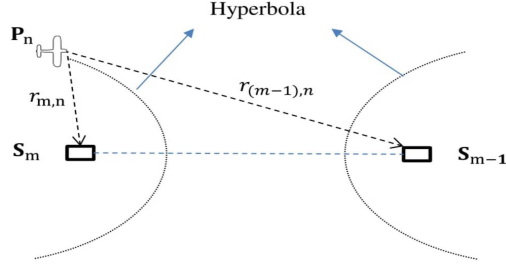


Fig. 4.1: Hyperbola made by TDOA measurements in two BSs located at \mathbf{S}_m and \mathbf{S}_{m-1} as foci and the target located at \mathbf{P}_n .

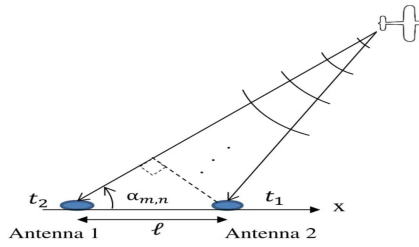


Fig. 4.2: The x-D antenna array of the m^{th} BS for measuring angle of arrival $\alpha_{m,n}$.

role of foci in a hyperbola and the BS is located on hyperbola. In order to find the unknown position of \mathbf{P}_n , AOA and TDOA measurements are gathered in matrix $\mathbf{k}_{m,n} \in \mathbb{R}^3$ as $\mathbf{k}_{m,n} \triangleq \begin{bmatrix} d_{m,(i,n)} & \mathbf{A}_{m,n}^T \end{bmatrix}$, where $\mathbf{A}_{m,n}$ is the same as in (8) and $d_{m,(i,n)}$ can be defined as

$$d_{m,(i,n)} = r_{m,n} - r_{m,i}. \quad (4.7)$$

where $r_{m,i}$ is the distance of the transmitter at the time instance t_i ($i < n$) from m^{th} BS. It is worth mentioning that m in this method, the PuOB, is one ($M = m = 1$), because only one BS is required.

The noisy version of $\mathbf{k}_{m,n}$, denotes as $\hat{\mathbf{k}}_{m,n}$ at the m^{th} BS is received as

$$\hat{\mathbf{k}}_{m,n} = \mathbf{k}_{m,n} + e, \quad (4.8)$$

where e is zero mean additive white Gaussian noise with the standard deviations of TDOA and two AOA measurements equal to $[\sigma_d \quad \sigma_\phi \quad \sigma_\theta]^T$, respectively .

By considering m^{th} BS and N measurement time instances, the measurements at the BS can be defined as $\mathbf{K} \triangleq \begin{bmatrix} \hat{\mathbf{k}}_{m,1} & \hat{\mathbf{k}}_{m,2} & \cdots & \hat{\mathbf{k}}_{m,N} \end{bmatrix} =$

$\left[\hat{d}_{m,(0,1)} \quad \hat{\mathbf{A}}_{m,1}^T \quad \cdots \quad \hat{d}_{m,(N-1,N)} \quad \mathbf{A}_{m,N}^T \right]$, where matrix $\mathbf{K} \in \mathbb{R}^N$ is the complete system measurements in m^{th} BS and all the time instances.

A matrix $\mathbf{G} \in \mathbb{R}^{3 \times 2}$ is defined in [46] in a way that its columns are an orthogonal basis of the plane orthogonal to the unit vector of the transmitter position with respect to the corresponding BS. We require a similar $\mathbf{G}_{m,n}$ to have

$$\mathbf{G}_{m,n}^T \mathbf{b}_{m,n} = 0, \quad (4.9)$$

where

$$\mathbf{G}_{m,n} = \begin{bmatrix} \sin \varphi_{m,n} & \cos \theta_{n,m} \cos \varphi_{n,m} \\ -\cos \varphi_{m,n} & \cos \theta_{m,n} \sin \varphi_{m,n} \\ 0 & -\sin \theta_{m,n} \end{bmatrix}. \quad (4.10)$$

Then, by substituting (4.4) for $\mathbf{b}_{m,n}$ in (4.9),

$$\mathbf{G}_{m,n}^T (\mathbf{P}_n - \mathbf{S}_m) = 0. \quad (4.11)$$

This results in

$$\mathbf{G}_{m,n}^T \mathbf{P}_n = \mathbf{G}_{m,n}^T \mathbf{S}_m. \quad (4.12)$$

Equation (4.12) can be written for any time instance, thus for t_i^{th} time instance,

$$\mathbf{G}_{m,i}^T \mathbf{P}_i = \mathbf{G}_{m,i}^T \mathbf{S}_m. \quad (4.13)$$

Adding (4.12) and (4.13) for two different time instances results

$$\mathbf{G}_{m,n}^T \mathbf{P}_n + \mathbf{G}_{m,i}^T \mathbf{P}_i = \mathbf{G}_{m,n}^T \mathbf{S}_m + \mathbf{G}_{m,i}^T \mathbf{S}_m. \quad (4.14)$$

For the time instances of t_n and t_i based on orthogonality of both $(\mathbf{b}_{m,n} - \mathbf{b}_{m,i})$ and $(\mathbf{b}_{m,n} + \mathbf{b}_{m,i})$ vectors [46] through (4.5), we have

$$r_{m,n}(\mathbf{b}_{m,n} - \mathbf{b}_{m,i})^T (\mathbf{b}_{m,n} + \mathbf{b}_{m,i}) = 0. \quad (4.15)$$

By using the expression of $r_{m,n}(\mathbf{b}_{m,n} + \mathbf{b}_{m,i})$ in (4.15) and $r_{m,n} = r_{m,i} + d_{m,(i,n)}$

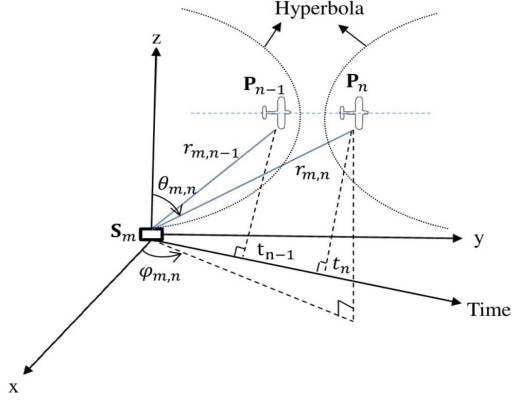


Fig. 4.3: The PuOB positioning of a target located at \mathbf{P}_n with one BS located at \mathbf{S}_m .

obtained from (4.7), we have

$$\begin{aligned} r_{m,n}(\mathbf{b}_{m,n} + \mathbf{b}_{m,i}) &= r_{m,n}\mathbf{b}_{m,n} + r_{m,n}\mathbf{b}_{m,i} \\ &= r_{m,n}\mathbf{b}_{m,n} + r_{m,i}\mathbf{b}_{m,i} + d_{m,(i,n)}\mathbf{b}_{m,i}. \end{aligned} \quad (4.16)$$

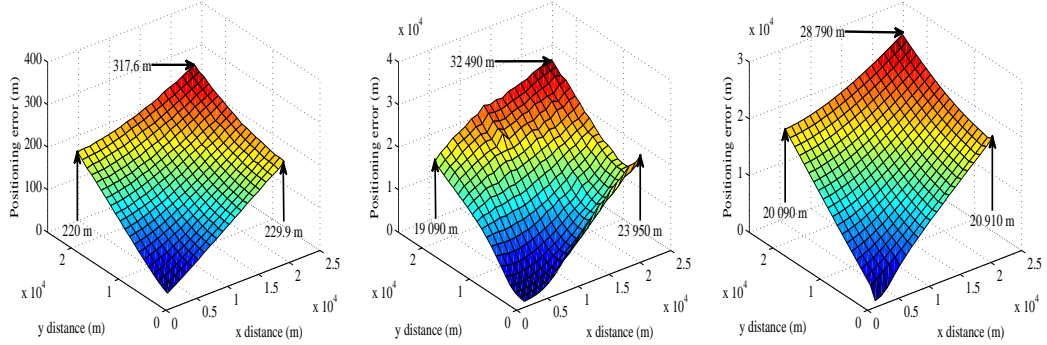
Equation (4.17) is achieved by substituting $r_{n,m}(\mathbf{b}_{m,n} + \mathbf{b}_{m,i})$ from (4.16) into (4.15)

$$\begin{aligned} &(\mathbf{b}_{m,n} - \mathbf{b}_{m,i})^T \left[\underbrace{r_{m,n}\mathbf{b}_{m,n}}_{\mathbf{P}_n - \mathbf{S}_m} + \underbrace{r_{m,i}\mathbf{b}_{m,i}}_{\mathbf{P}_i - \mathbf{S}_m} + d_{m,(i,n)}\mathbf{b}_{m,i} \right] \\ &= (\mathbf{b}_{m,n} - \mathbf{b}_{m,i})^T [\mathbf{P}_n + \mathbf{P}_i - 2\mathbf{S}_m + d_{m,(i,n)}\mathbf{b}_{m,i}] = 0. \end{aligned} \quad (4.17)$$

Therefore:

$$\begin{aligned} &(\mathbf{b}_{m,n} - \mathbf{b}_{m,i})^T (\mathbf{P}_n + \mathbf{P}_i) = \\ &(\mathbf{b}_{m,n} - \mathbf{b}_{m,i})^T (2\mathbf{S}_m - d_{m,(i,n)}\mathbf{b}_{m,i}). \end{aligned} \quad (4.18)$$

Equations (4.14) and (4.18) define the necessary equations for PuOB estimation. Estimated multiplier matrix of unknown transmitter position at time instance t_n is denoted by $\hat{\mathbf{F}}_{m,n} \in \mathbb{R}^{3 \times 3}$ which can be extracted from (4.14) and



(a) PuOB method with $U_i = U_0$. (b) AOA method using two BSs. (c) TAP method using two BSs.

Fig. 4.4: Average localization error of PuOB, AOA and TAP methods, for different x,y locations of a target. (The height of the target, σ_{TDOA} and $[\sigma_\phi \ \sigma_\theta]^T$ are set to 1000 m, 30 ns and $[0.5 \ 0.5]^T$ degrees, respectively.)

(4.18)

$$\hat{\mathbf{F}}_{m,n} = \begin{bmatrix} (\hat{\mathbf{b}}_{m,n} - \hat{\mathbf{b}}_{m,i})^T \\ \hat{\mathbf{G}}_{m,n}^T \end{bmatrix}, \quad (4.19)$$

and similarly $\hat{\mathbf{F}}_{m,i}$ for known transmitter position at time instance t_i . Then we will have:

$$\hat{\mathbf{F}}_{m,n} \hat{\mathbf{P}}_n + \hat{\mathbf{F}}_{m,i} \hat{\mathbf{P}}_i = \hat{\mathbf{D}}, \quad (4.20)$$

where $\hat{\mathbf{D}} \in \mathbb{R}^3$ using (4.14) and (4.18) is obtained as

$$\hat{\mathbf{D}} = \begin{bmatrix} (\hat{\mathbf{b}}_{m,n} - \hat{\mathbf{b}}_{m,i})^T (2\mathbf{S}_m - \hat{d}_{m,(i,n)} \hat{\mathbf{b}}_{m,i}) \\ \hat{\mathbf{G}}_{m,n}^T \mathbf{S}_m + \hat{\mathbf{G}}_{m,i}^T \mathbf{S}_m \end{bmatrix}. \quad (4.21)$$

Finally, the estimated position of the transmitter can be obtained from:

$$\hat{\mathbf{P}}_n = \hat{\mathbf{F}}_{m,n}^{-1} \left(\hat{\mathbf{D}} - \hat{\mathbf{F}}_{m,i} \hat{\mathbf{P}}_i \right). \quad (4.22)$$

Note that in (4.19) to (4.22), $(\hat{\cdot})$ denotes the estimated values obtained from the measurements.

4.2 Performance Evaluation

In this section, we compare the performance of the PuOB method utilizing one BS with AOA and TAP methods utilizing two BSs in order to have a fair comparison according to the least number of BSs. In AOA and TAP methods the BSs are located in 400 meters apart from each other, the same distance as it is common in urban cellular networks ($\mathbf{S}_1 = [0 \ 0 \ 0]^T$ and $\mathbf{S}_2 = [400 \ 0 \ 0]^T$ meters). The BS used in PuOB is located at $\mathbf{S}_1 = [0 \ 0 \ 0]^T$. We consider four simulation scenarios. In the first two, the location of the transmitter is varied in order to observe the performance of the methods in terms of distance between transmitter and BSs. During the first simulation scenario, position of the transmitter is varied from $\mathbf{P}_0 = [1\ 000 \ 1\ 000 \ 1\ 000]^T$ meters till $\mathbf{P}_N = [20\ 000 \ 20\ 000 \ 1\ 000]^T$ meters. $\sigma_{TDOA} = \sigma_d/c$ denotes the standard deviation of time difference of arrival measurements and it is assumed to be 30 ns with respect to the distance between BSs in urban cellular networks and $[\sigma_\phi \ \sigma_\theta]^T$ are set to $[0.5 \ 0.5]^T$ degrees based on the range of signal diffraction in [46]. Figs. 4(a), (b) and (c) show the average error performance of PuOB, AOA and TAP methods based on different positions of transmitter. The results present that PuOB and TAP methods are more stable than AOA method with respect to the position of transmitter. The AOA method estimation highly depends on the position of transmitter with respect to the position of BSs. It is shown that $\sigma_{\phi,\theta} = 0.5$ degree in pure AOA method leads to large error in far distances. As shown in Fig. 4(b), the estimation in x-direction, where two BSs are located, is getting worse because of narrowness and similarity of the AOA measurements in both BSs. But in y-direction it has better performance than x-direction because of having different and clear angles in two BSs located in x-axis. Both of the PuOB and TAP methods are more symmetric and stable in different angles due to the nature of using hybrid AOA and TDOA measurements. In fact, TDOA measurements in PuOB and TAP can decrease the dependency on AOA measurements; however, TAP method utilizes more AOA measurements than PuOB causing more dependency on AOA measurements than PuOB. In addition, in case of GDP problem, PuOB outperforms two other methods. At maximum distance, average error observed by PuOB is 317.6 m, while in AOA and TAP methods, average errors reach up to 32 km and

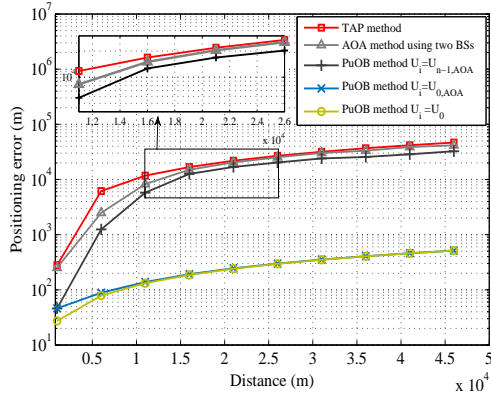


Fig. 4.5: Performance comparison of PuOB with different initializations, AOA and TAP localizations of a target located in y-axis while BSs are located in x-axis.

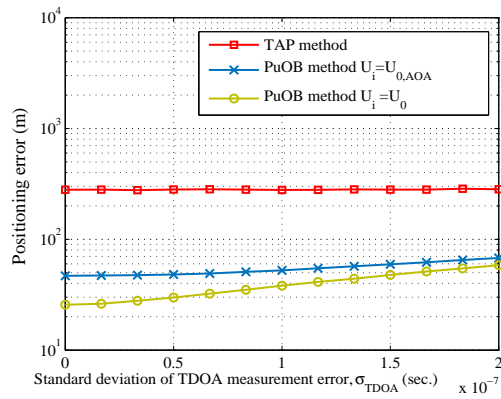


Fig. 4.6: The effect of σ_{TDOA} variation on the performance of PuOB, AOA and TAP methods.

28 km, receptively.

In the second scenario, the PuOB method is initialized with three different initial positions (\mathbf{P}_i). The transmitter's position is varied in y-direction and other parameters such as σ_{TDOA} and $[\sigma_\phi \ \sigma_\theta]^T$ are the same as the first scenario. In other words, this simulation shows what Fig. 4 provides in y-direction with different initializations in PuOB. Three different initial transmitter's positions are: I The exact position of transmitter at t_0 , ($\mathbf{P}_i = \mathbf{P}_0$), II The estimated position of transmitter by AOA method at t_0 ($\mathbf{P}_i = \mathbf{P}_{0, AOA}$), III The estimated position of transmitter by AOA method at t_{n-1} , ($\mathbf{P}_i = \mathbf{P}_{n-1, AOA}$). As shown in Fig. 5, with all three initial positions, the PuOB method outperforms other

methods considered in this work. According to results, if the distance between the initial position and intended position is more than 5000 m, the dependency of PuOB estimation on initial position will be reduced. Furthermore, as mentioned in first scenario, AOA method performs slightly better than TAP method in y-axis positioning because of clear AOA measurements of transmitter at BSs located in x-axis. However, Figs. 4 (b) and (c) show that TAP method performs better than AOA method generally.

In the third scenario, we assume that σ_{TDOA} is variable while the locations and $[\sigma_\phi \ \sigma_\theta]^T$ are fixed.

σ_{TDOA} is varied from 0 to 200 ns to observe the performance of the PuOB method and TAP methods. The location of the transmitter is fixed in $\mathbf{P}_n = [2000 \ 1000 \ 1000]^T$ and \mathbf{P}_0 is set to $[1000 \ 1000 \ 1000]^T$. $[\sigma_\phi \ \sigma_\theta]^T$ are fixed as $[0.5 \ 0.5]^T$ degrees. Two cases of initializations are considered like the first two initializations in the second scenario. First, $\mathbf{P}_i = \mathbf{P}_0$ and second, $\mathbf{P}_i = \mathbf{P}_{0,AOA}$. Fig. 6 depicts that the PuOB method with both of initialization procedures outperforms TAP method. Even if PuOB method is initialized by erroneous position obtained by AOA estimation, its performance approaches to the estimations initialized by the exact position of the transmitter. Furthermore, TAP method results in a relatively constant error performance in low variations of σ_{TDOA} due to its low dependency on TDOA measurements.

The last scenario is reserved to study the effect of $[\sigma_\phi \ \sigma_\theta]^T$ variations on the performance of localization methods. We assume $[\sigma_\phi \ \sigma_\theta]^T$ vary from 0.25 degrees to 5 degrees. σ_{TDOA} is set to 30 ns. The position of the transmitter and initial positions (\mathbf{P}_i) are the same as the third scenario. As shown in Fig. 7, PuOB method outperforms AOA and TAP methods. It is worth mentioning that both of the initialized PuOB estimation cases approach to each other in high $[\sigma_\phi \ \sigma_\theta]^T$ variations. Furthermore, the TAP method outperforms AOA method after $[\sigma_\phi \ \sigma_\theta]^T = [1 \ 1]^T$ degrees.

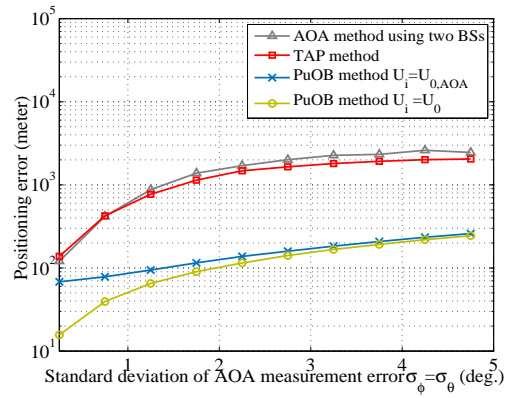


Fig. 4.7: The effect of $[\sigma_\phi \ \sigma_\theta]^T$ variations on the performance of PuOB, AOA and TAP methods ($\sigma_\phi = \sigma_\theta$).

Chapter 5

Concluding Remarks

5.1 Summary

In this dissertation, we investigated the design of new waveform design and new symbol boundary alignment to avoid the drawbacks of current waveform and symbol boundary alignment in 5G.

In chapter ??, we proposed Two flexible waveform in terms of CP length (guard interval). The proposed waveforms have lower PAPR and OOB in comparison to OFDM. In DFT-s- ZW OFDM the ISI problem of ZT DFT-s-OFDM is solved. Thus, the highlight features of the waveform is adaptive ZW and lower ISI in dsipersive channels. We also proposed a hybrid waveform which is a co-existence waveform of ZT DFT-s-OFDM and DFT-s ZW OFDM. The hybrid waveform has the advantages of both but can avoid disadvantages of them.

In chapter 3, a novel genetic algorithm-based method is proposed to optimize the resource allocation and power assignment of D2D communication underlying cellular communication. Contrary to orthogonal resource allocation and GAAM, the algorithm is presented with respect to the flexible number of D2D and cellular communications. Therefore, larger number of users can be served with a limited

number of resource blocks. Also, a minimum SINR is considered for the cellular communications to guarantee the quality of service of them. Moreover, despite GAAM, operators of the genetic algorithm are defined to produce an acceptable offspring at each iteration. Therefore, no additional randomness is added to the algorithm. It results in superior performance and fast converging of the proposed method compared to GAAM.

Finally, in chapter 4, a simple and linear positioning method, namely PuOB is introduced, which requires only one base station to track the location of mobile transmitters. Simulation results indicate that PuOB with one base station has superior positioning performance than the angle-of-arrival and hybrid time and angle of arrival methods with two base stations. Additionally, PuOB is robust against errors in angle and time measurements.

Bibliography

- [1] A. Algedir and H. H. Refai. Adaptive d2d resources allocation underlying (2-tier) heterogeneous cellular networks. In *2017 IEEE 28th Annual International Symposium on Personal, Indoor, and Mobile Radio Communications (PIMRC)*, pages 1–6, Oct 2017.
- [2] Mudassar Ali, Saad Qaisar, Muhammad Naeem, and Shahid Mumtaz. Energy efficient resource allocation in d2d-assisted heterogeneous networks with relays. *IEEE Access*, 4:4902–4911, 2016.
- [3] Alan John Anderson. Channel prediction in wireless communications. 2015.
- [4] Arash Asadi, Qing Wang, and Vincenzo Mancuso. A survey on device-to-device communication in cellular networks. *IEEE Communications Surveys & Tutorials*, 16(4):1801–1819, 2014.
- [5] Oladayo Bello and Sherali Zeadally. Intelligent device-to-device communication in the internet of things. *IEEE Systems Journal*, 10(3):1172–1182, 2016.
- [6] Gilberto Berardinelli, Klaus I Pedersen, Troels B Sorensen, and Preben Mogenssen. Generalized dft-spread-ofdm as 5g waveform. *IEEE Communications Magazine*, 54(11):99–105, 2016.
- [7] Adrian N Bishop, Barış Fidan, Kutluyıl Doğançay, Brian DO Anderson, and Pubudu N Pathirana. Exploiting geometry for improved hybrid aoa/tdoa-based localization. *Signal Processing*, 88(7):1775–1791, 2008.

- [8] Xianghui Cao, Lu Liu, Yu Cheng, Lin X Cai, and Changyin Sun. On optimal device-to-device resource allocation for minimizing end-to-end delay in vanets. *IEEE Transactions on Vehicular Technology*, 65(10):7905–7916, 2016.
- [9] Shanzhi Chen and Jian Zhao. The requirements, challenges, and technologies for 5g of terrestrial mobile telecommunication. *IEEE Communications Magazine*, 52(5):36–43, 2014.
- [10] Yong Soo Cho, Jaekwon Kim, Won Young Yang, and Chung G Kang. *MIMO-OFDM wireless communications with MATLAB*. John Wiley & Sons, 2010.
- [11] Kalyanmoy Deb. *Multi-objective optimization using evolutionary algorithms*, volume 16. John Wiley & Sons, 2001.
- [12] Haichuan Ding, Shaodan Ma, and Chengwen Xing. Feasible d2d communication distance in d2d-enabled cellular networks. In *Communication Systems (ICCS), 2014 IEEE International Conference on*, pages 1–5. IEEE, 2014.
- [13] Klaus Doppler, Mika Rinne, Carl Wijting, Cássio B Ribeiro, and Klaus Hugl. Device-to-device communication as an underlay to lte-advanced networks. *IEEE Communications Magazine*, 47(12), 2009.
- [14] Alexandra Duel-Hallen. Fading channel prediction for mobile radio adaptive transmission systems. *Proceedings of the IEEE*, 95(12):2299–2313, 2007.
- [15] Alexandra Duel-Hallen, Hans Hallen, and Tung-Sheng Yang. Long range prediction and reduced feedback for mobile radio adaptive ofdm systems. *IEEE Transactions on Wireless Communications*, 5(10):2723–2733, 2006.
- [16] Alexandra Duel-Hallen, Shengquan Hu, and Hans Hallen. Long range prediction of fading signals: Enabling adaptive transmission for mobile radio channels1.
- [17] Torbjörn Ekman. *Prediction of mobile radio channels: modeling and design*. PhD thesis, Institutionen för materialvetenskap, 2002.

- [18] Tugay Eyceoz, Alexandra Duel-Hallen, and Hans Hallen. Deterministic channel modeling and long range prediction of fast fading mobile radio channels. *IEEE Communications Letters*, 2(9):254–256, 1998.
- [19] Behrouz Farhang-Boroujeny. Ofdm versus filter bank multicarrier. *IEEE signal processing magazine*, 28(3):92–112, 2011.
- [20] Fredrik Gustafsson and Fredrik Gunnarsson. Positioning using time-difference of arrival measurements. In *Acoustics, Speech, and Signal Processing, 2003. Proceedings.(ICASSP'03). 2003 IEEE International Conference on*, volume 6, pages VI–553. IEEE, 2003.
- [21] Yeakub Hassan, Faisal Hussain, Sakhawat Hossen, Salimur Choudhury, and Muhammad Mahbub Alam. Interference minimization in d2d communication underlying cellular networks. *IEEE Access*, 5:22471–22484, 2017.
- [22] Pekka Janis, Visa Koivunen, Cassio Ribeiro, Juha Korhonen, Klaus Doppler, and Klaus Hugl. Interference-aware resource allocation for device-to-device radio underlying cellular networks. In *Vehicular Technology Conference, 2009. VTC Spring 2009. IEEE 69th*, pages 1–5. IEEE, 2009.
- [23] Sangdeok Kim and Jong-Wha Chong. An efficient tdoa-based localization algorithm without synchronization between base stations. *International Journal of Distributed Sensor Networks*, 11(9):832351, 2015.
- [24] Wen-Yang Lin, Wen-Yung Lee, and Tzung-Pei Hong. Adapting crossover and mutation rates in genetic algorithms. *J. Inf. Sci. Eng.*, 19(5):889–903, 2003.
- [25] Xingqin Lin, Jeffrey G Andrews, and Amitava Ghosh. Spectrum sharing for device-to-device communication in cellular networks. *IEEE Transactions on Wireless Communications*, 13(12):6727–6740, 2014.
- [26] Rui Liu, Guanding Yu, Fengzhong Qu, and Zihan Zhang. Device-to-device communications in unlicensed spectrum: Mode selection and resource allocation. *IEEE Access*, 4:4720–4729, 2016.

- [27] Juha Meinilä, Pekka Kyösti, Tommi Jämsä, and Lassi Hentilä. Winner ii channel models. *Radio Technologies and Concepts for IMT-Advanced*, pages 39–92, 2009.
- [28] Y Norouzi and M Derakhshani. Joint time difference of arrival/angle of arrival position finding in passive radar. *IET radar, sonar & navigation*, 3(2):167–176, 2009.
- [29] Afif Osseiran, Federico Boccardi, Volker Braun, Katsutoshi Kusume, Patrick Marsch, Michal Maternia, Olav Queseth, Malte Schellmann, Hans Schotten, Hidekazu Taoka, et al. Scenarios for 5g mobile and wireless communications: the vision of the metis project. *IEEE Communications Magazine*, 52(5):26–35, 2014.
- [30] Neal Patwari, Joshua N Ash, Spyros Kyperountas, Alfred O Hero, Randolph L Moses, and Neiyer S Correal. Locating the nodes: cooperative localization in wireless sensor networks. *IEEE Signal processing magazine*, 22(4):54–69, 2005.
- [31] Kambam Suresh Kumar Reddy, D Rajaveerappa, and S Khadeeja Banu. Two base station method for finding location of mobile vehicles based on doppler shifted signals. In *Emerging Trends in Communication, Control, Signal Processing & Computing Applications (C2SPCA), 2013 International Conference on*, pages 1–8. IEEE, 2013.
- [32] Peng Rong and Mihail L Sichitiu. Angle of arrival localization for wireless sensor networks. In *Sensor and Ad Hoc Communications and Networks, 2006. SECON'06. 2006 3rd Annual IEEE Communications Society on*, volume 1, pages 374–382. IEEE, 2006.
- [33] Ahmed Hamdi Sakr, Hina Tabassum, Ekram Hossain, and Dong In Kim. Cognitive spectrum access in device-to-device-enabled cellular networks. *IEEE Communications Magazine*, 53(7):126–133, 2015.
- [34] Frank Schaich, Thorsten Wild, and Yejian Chen. Waveform contenders for 5g-suitability for short packet and low latency transmissions. In *Vehicular*

- Technology Conference (VTC Spring), 2014 IEEE 79th*, pages 1–5. IEEE, 2014.
- [35] S Series. Comparison of time-difference-of-arrival and angle-of-arrival methods of signal geolocation. 2011.
- [36] Lingyang Song, Dusit Niyato, Zhu Han, and Ekram Hossain. Game-theoretic resource allocation methods for device-to-device communication. *IEEE Wireless Communications*, 21(3):136–144, 2014.
- [37] Mohsen Nader Tehrani, Murat Uysal, and Halim Yanikomeroglu. Device-to-device communication in 5g cellular networks: challenges, solutions, and future directions. *IEEE Communications Magazine*, 52(5):86–92, 2014.
- [38] Feiran Wang, Lingyang Song, Zhu Han, Qun Zhao, and Xiaoli Wang. Joint scheduling and resource allocation for device-to-device underlay communication. In *Wireless Communications and Networking Conference (WCNC), 2013 IEEE*, pages 134–139. IEEE, 2013.
- [39] Feiran Wang, Chen Xu, Lingyang Song, and Zhu Han. Energy-efficient resource allocation for device-to-device underlay communication. *IEEE Transactions on Wireless Communications*, 14(4):2082–2092, 2015.
- [40] Feiran Wang, Chen Xu, Lingyang Song, Qun Zhao, Xiaoli Wang, and Zhu Han. Energy-aware resource allocation for device-to-device underlay communication. In *Communications (ICC), 2013 IEEE International Conference on*, pages 6076–6080. IEEE, 2013.
- [41] Thorsten Wild, Frank Schaich, and Yejian Chen. 5g air interface design based on universal filtered (uf-) ofdm. In *Digital Signal Processing (DSP), 2014 19th International Conference on*, pages 699–704. IEEE, 2014.
- [42] Ian C Wong, Antonio Forenza, Robert W Heath, and Brian L Evans. Long range channel prediction for adaptive ofdm systems. In *Signals, Systems and Computers, 2004. Conference Record of the Thirty-Eighth Asilomar Conference on*, volume 1, pages 732–736. IEEE, 2004.

- [43] Bin Xu, Guodong Sun, Ran Yu, and Zheng Yang. High-accuracy tdoa-based localization without time synchronization. *IEEE Transactions on Parallel and Distributed Systems*, 24(8):1567–1576, 2013.
- [44] Chen Xu, Lingyang Song, Zhu Han, Qun Zhao, Xiaoli Wang, and Bingli Jiao. Interference-aware resource allocation for device-to-device communications as an underlay using sequential second price auction. In *Communications (ICC), 2012 IEEE International Conference on*, pages 445–449. IEEE, 2012.
- [45] Chengcheng Yang, Xiaodong Xu, Jiang Han, Waheed ur Rehman, and Xiaofeng Tao. Ga based optimal resource allocation and user matching in device to device underlaying network. In *Wireless Communications and Networking Conference Workshops (WCNCW), 2014 IEEE*, pages 242–247. IEEE, 2014.
- [46] Jihao Yin, Qun Wan, Shiwen Yang, and KC Ho. A simple and accurate tdoa-aoa localization method using two stations. *IEEE Signal Processing Letters*, 23(1):144–148, 2016.
- [47] Chia-Hao Yu, Klaus Doppler, Cassio B Ribeiro, and Olav Tirkkonen. Resource sharing optimization for device-to-device communication underlaying cellular networks. *IEEE Transactions on Wireless communications*, 10(8):2752–2763, 2011.
- [48] Chia-Hao Yu, Olav Tirkkonen, Klaus Doppler, and Cássio Ribeiro. On the performance of device-to-device underlay communication with simple power control. In *Vehicular Technology Conference, 2009. VTC Spring 2009. IEEE 69th*, pages 1–5. IEEE, 2009.
- [49] Guanding Yu, Lukai Xu, Daquan Feng, Rui Yin, Geoffrey Ye Li, and Yuhuan Jiang. Joint mode selection and resource allocation for device-to-device communications. *IEEE transactions on communications*, 62(11):3814–3824, 2014.
- [50] Hongliang Zhang, Yun Liao, and Lingyang Song. Device-to-device communications over unlicensed spectrum. *Handbook of Cognitive Radio*, pages 1–30, 2017.

- [51] Xiguang Zhang, Yong Shang, Xiaobo Li, and Jiayi Fang. Research on overlay d2d resource scheduling algorithms for v2v broadcast service. In *Vehicular Technology Conference (VTC-Fall), 2016 IEEE 84th*, pages 1–5. IEEE, 2016.
- [52] Wei Zhong, Yixin Fang, Shi Jin, Kai-Kit Wong, Sheng Zhong, and Zuping Qian. Joint resource allocation for device-to-device communications underlying uplink mimo cellular networks. *IEEE Journal on Selected Areas in Communications*, 33(1):41–54, 2015.
- [53] Chunsheng Zhu, Victor CM Leung, Lei Shu, and Edith C-H Ngai. Green internet of things for smart world. *IEEE Access*, 3:2151–2162, 2015.
- [54] Mohammad Zulhasnine, Changcheng Huang, and Anand Srinivasan. Efficient resource allocation for device-to-device communication underlying lte network. In *Wireless and Mobile Computing, Networking and Communications (WiMob), 2010 IEEE 6th International Conference on*, pages 368–375. IEEE, 2010.
- [55] Jim Zyren and Wes McCoy. Overview of the 3gpp long term evolution physical layer. *Freescale Semiconductor, Inc., white paper*, 2007.

5G CHALLENGES : WAVEFORM DESIGN AND D2D COMMUNICATION

ORIGINALITY REPORT

14%

SIMILARITY INDEX

8%

INTERNET SOURCES

11%

PUBLICATIONS

3%

STUDENT PAPERS

MATCH ALL SOURCES (ONLY SELECTED SOURCE PRINTED)

2%

★ etd.lib.metu.edu.tr

Internet Source

Exclude quotes Off

Exclude matches Off

Exclude bibliography On